SHORT-TERM CARM1 INHIBITION AND SKELETAL MUSCLE BIOLOGY

EFFECTS OF SHORT-TERM, PHARMACOLOGICAL CARM1 INHIBITION ON SKELETAL MUSCLE MASS, FUNCTION, AND ATROPHY

By ERIN WEBB, B.Sc. Kin Honours

A Thesis Submitted to the School of Graduate Studies in Partial Fulfilment of the Requirements for the Degree Master of Science

McMaster University MASTER OF SCIENCE (2022) Hamilton, Ontario (Kinesiology)

TITLE: Effects of short-term, pharmacological CARM1 inhibition on skeletal muscle mass, function, and atrophy

AUTHOR: Erin Webb, B.Sc. Kin Honours (McMaster University)

SUPERVISOR: Dr. Vladimir Ljubicic, PhD

NUMBER OF PAGES: viii, 85

Lay Abstract

Coactivator-associated arginine methyltransferase 1 (CARM1) is an enzyme that alters the activity of other proteins. CARM1 plays an important role in several tissues, however, little is understood about its function in skeletal muscle. Recent research suggests that CARM1 could be involved in the process of skeletal muscle wasting and weakness, termed muscle atrophy. Therefore, we aimed to study the effects of short-term pharmacological CARM1 inhibition on skeletal muscle mass, function, and atrophy in adult mice. Our observations show that treatment with a CARM1-inhibiting compound was very effective at reducing CARM1 activity in muscle. CARM1 inhibition did not affect muscle mass, but it did decrease muscular endurance, particularly in male mice. Suppressed CARM1 activity had no impact on muscle wasting or molecular atrophy signalling following a period of denervation-evoked muscle disuse. Collectively, we demonstrate that short-term CARM1 inhibition impacts muscle performance without affecting the maintenance and plasticity of muscle mass.

Abstract

Coactivator-associated arginine methyltransferase 1 (CARM1) catalyzes the methylation of arginine residues on target proteins critical for health and disease. The purpose of this study was to characterize the effects of short-term, pharmacological CARM1 inhibition on skeletal muscle size, function, and atrophy. Adult mice (n = 10-11/sex) were treated with either a CARM1 inhibitor (150 mg/kg EZM2302; EZM) or vehicle (Veh) via oral gavage for 11-13 days and muscle mass, function, and exercise capacity were assessed. Additionally, we investigated the effect of CARM1 suppression on unilateral hindlimb denervation (DEN)-induced muscle atrophy (n = 8/sex). We report that CARM1 inhibition caused significant reductions in the asymmetric dimethylation of known CARM1 substrates but no change in CARM1 protein or mRNA content in skeletal muscle. Reduced CARM1 activity did not affect body or muscle mass, however, we observed a decrease in exercise capacity and muscular endurance in male mice. CARM1 methyltransferase activity increased in the muscle of Veh-treated mice following 7 days of DEN and this response was blunted in EZM-dosed mice. Skeletal muscle mass and myofiber cross-sectional area were significantly reduced in DEN compared to contralateral, non-DEN limbs to a similar degree in both treatment groups. Furthermore, skeletal muscle atrophy and autophagy gene expression programs were elevated in response to DEN independent of CARM1 suppression. Collectively, these results suggest that short-term, pharmacological CARM1 inhibition in adult animals affects muscle performance in a sex-specific manner but does not impact the maintenance and remodeling of skeletal muscle mass during conditions of neurogenic muscle atrophy.

Acknowledgements

To the members of the Integrative Neuromuscular Biology Lab, thank you for your support. Derek, thank you for teaching me the art of denervation surgery and for being such a kind mentor. Tiffany, thank you for guiding me through the functional tests and for your words of encouragement along the way. Sean, thank you for very patiently teaching me how to gavage a mouse, helping me navigate through my experiments, and always answering my questions with kindness and expertise. Andrew, thank you for your continuous help with lab work, your guidance through the analysis and writing process, and for always joining me for coffee breaks. Steph and Rozhin, thank you for being the best conference roommates and for making the time in the lab and CAF so enjoyable.

To the "EB Crew", Mike, Magda, and Aidan, thank you for the science chats and for all the post-lab socials. To my friend and roommate, Michelle, thank you for sharing your baking with me and for giving the best advice.

To the Exercise Metabolism Research Group, thank you for creating such an enjoyable, productive work environment. I would also like to thank Todd and Linda for sharing their expertise and providing technical assistance.

To Dr. Baraa Al-Khazraji, Dr. Gianni Parise, and Dr. Irena Rebalka, thank you for serving on my supervisory committee and sharing your academic expertise. I am grateful for your feedback and contributions towards this study.

To my parents, friends, and family, thank you for your continuous love and support, and for regularly checking in on me and "my mice". Noah, thank you for being such a source of joy, sharing your optimistic energy with me, and being my #1 supporter.

Finally, thank you to my supervisor Vlad. Thank you for guiding me through the first year of my degree in the middle of a pandemic, providing me with countless opportunities to grow as a researcher, and supporting me in my decision to pursue teaching. I really appreciate your guidance and mentorship over the last 2 years.

Table of Contents

List of Figures

Review of the Literature Figures

Manuscript Figures

List of Abbreviations

ADMA – asymmetric dimethylarginine

ADP – Adenosine diphosphate

AMPK – AMP-activated protein kinase

ATP – Adenosine triphosphate

BAF155 – SWI/SNF chromatin remodeling complex BAF155

Bnip3 – BCL2 interacting protein 3

CARM1 – Coactivator-associated arginine methyltransferase 1

CN – Calcineurin

FGFBP1 – Fibroblast growth factor-binding protein

FOXO – Forkhead box O

kDa – Kilodalton

LC3 – microtubule-associated protein 1A/1B-light chain 3

MAFbx – Muscle atrophy F-box

MEF-2C – Myocyte enhancer factor-2C

MHC – Myosin heavy chain

MMA – Monomethylarginine

mTORC1 – Mammalian target of rapamycin complex 1

MuRF1 – Muscle RING finger 1

NEDD4 – Developmentally down-regulated protein 4

OXPHOS – Complexes I-V of mitochondrial oxidative phosphorylation

PABP1 – Poly(A)-binding protein 1

PGC-1α – Peroxisome proliferator-activated receptor-γ coactivator-1α

PRMT – Protein arginine methyltransferase

p38 – p38 mitogen-activated protein kinase

p62 – Sequestosome 1

SAM – S-adenosylmethionine

SDMA – Symmetric dimethylarginine

s6 – Ribosomal protein s6

ULK – unc-51-like kinase

4EBP1 – 4E-binding protein-1

Review of the Literature

1. Skeletal muscle

1.1: Introduction to skeletal muscle

Skeletal muscle comprises approximately 40% of total body weight and contains 50-75% of all body proteins in mammals (Frontera & Ochala, 2015). In addition to its role in locomotion and posture, skeletal muscle is essential for the regulation of whole-body metabolism, maintenance of core temperature, and serving as the body's reservoir for amino acids (Baskin et al., 2015). Skeletal muscle also releases myokines and metabolites that may facilitate exercise-induced adaptations in other body tissues, such as the brain and liver (Delezie & Handschin, 2018). The remarkable plasticity of skeletal muscle in response to various stressors, such as exercise and disease, renders it vital for organismal health and survival. Indeed, in conditions where skeletal muscle mass and function are compromised, such as cancer cachexia and sarcopenia, there is an associated decrease in lifespan (Baskin et al., 2015; Kalyani et al., 2014). It is therefore critical to improve our understanding of the intricacies of skeletal muscle biology. In this review, we will discuss the morphology and cellular biology of skeletal muscle and outline the mechanisms that contribute to skeletal muscle atrophy with a focus on the role of coactivator-associated arginine methyltransferase (CARM1).

Skeletal muscle is made up of hundreds to thousands of multinucleated and highly vascularized cells, called muscle fibres, that extend the entire length of the muscle. Each muscle fibre is enveloped by the sarcolemma and contains hundreds to thousands of myofibrils. The myofibril is composed of myofilaments that form sarcomeres; the smallest contractile unit of the muscle. Also within each muscle fibre is a network of transverse

tubules that propagate electrical impulses deep into the muscle to ultimately trigger contraction (Block et al., 1988). Additionally, mitochondria are located throughout the sarcoplasm and within the intermyofibrillar space to generate the energy needed for muscle contraction (Dahl et al., 2015). In healthy, developed skeletal muscle fibres, myonuclei are located at the periphery of the fibre and meet the transcriptional demand in the surrounding region, referred to as the myonuclear domain (Cadot et al., 2015). Within the skeletal muscle, several other cell types exist. For instance, muscle stem cells or satellite cells typically reside between the sarcolemma and basal lamina; adjacent to myonuclei (Mauro, 1961). When activated by myogenic factors or mechanical stimuli, satellite cells proliferate and/or differentiate into myoblasts that fuse together to form new muscle fibres or into existing fibres to allow the muscle to grow, repair, and regenerate in response to damaging conditions (Snijders et al., 2015). Moreover, infiltrations of adipocytes and connective tissue are also present within skeletal muscle (Purslow, 2020; Vettor et al., 2009).

A muscle contraction is initiated when an action potential arrives at the neuromuscular junction, triggering the release of acetylcholine (ACh) from the motor end plate into the synaptic cleft (Bagshaw, 1993). ACh initiates depolarization within the sarcolemma and spreads into the transverse tubules that project into the interior of the muscle fibre. The depolarization of the tubules triggers the release of calcium ions from the sarcoplasmic reticulum. Upon release, calcium ions bind troponin found on the actin filament, causing the displacement of tropomyosin which exposes the active site of actin (Zot & Potter, 1987). The myosin heads are then able to bind to actin to form cross bridges and use stored energy to pull actin towards the centre of the sarcomere, releasing adenosine

diphosphate (ADP) simultaneously. Next, adenosine triphosphate (ATP) attaches to the myosin head and causes its release from actin. When the ATP is hydrolyzed, the myosin head returns to its resting position. If calcium ions remain bound to tropomyosin, the cross-bridge cycling is repeated (Fitts, 2008). Altogether, the collective and continuous shortening of the sarcomeres within each myofibril through excitation-contraction coupling induces skeletal muscle contraction.

1.2: Skeletal muscle plasticity

There are four unique types of fibres in murine skeletal muscle: Type I, IIa, IIx, and IIb. Each muscle fibre type has unique properties and can be classified based on the expression of different myosin heavy chain (MHC) isoforms, contractile speed, and metabolic capacity (Zierath & Hawley, 2004). Type 1 fibres express MHCI, have slow contractile speed, and primarily rely on oxidative metabolism (Schiaffino, 2010). The three different type II fibres (expressing MHCIIa, MHCIIx, and MHCIIb) vary in their contractile speed and metabolic capacity. Type IIa fibres are slow twitch and more oxidative, whereas, type IIb have the fastest contractile speed and are the most glycolytic, and type IIx are an intermediate between IIa and IIb (Schiaffino, 2010). Additionally, a shift in the predominant MHC profile within a fibre can allow it to express two isoforms of MHC simultaneously, termed hybrid fibres (e.g.: MHCI and MHCIIa) (Staron & Pette, 1993). The heterogeneity that exists between skeletal muscles within the body is partially due to the unique distribution of the fibre types within each muscle. For example, the proportion of type I, IIa, IIx, IIb, and hybrid fibres in murine gastrocnemius (GAST) is: 0%, 21%, 15%, 56%, and 8%, compared to the soleus (SOL): 31%, 49%, 12%, 5%, and

3% (Bloemberg & Quadrilatero, 2012). Importantly, these distributions are approximations and can fluctuate under various conditions of skeletal muscle remodeling.

Skeletal muscle is a uniquely malleable tissue that can adapt to different stimuli. For instance, chronic endurance exercise can induce a shift towards a slower, more oxidative profile with a larger percentage of type I and IIa fibres (Blaauw et al., 2013). By contrast, prolonged muscle disuse typically causes a shift towards a faster, more glycolytic phenotype (Ciciliot et al., 2013). The maintenance of the skeletal muscle phenotype is dependent on the coordination of several intracellular signalling pathways that govern cellular processes. Notably, peroxisome proliferator-activated receptor-γ coactivator-1α (PGC-1α), a transcriptional co-activator, is well-known as the master regulator of mitochondrial biogenesis (Fernandez-Marcos & Auwerx, 2011). PGC-1α is involved in the regulation of nuclear and mitochondrial genes responsible for shifting a fibre towards a more oxidative phenotype (Ljubicic et al., 2014). The overexpression of PGC-1α causes a dramatic increase in the proportion of type I fibres, greater mitochondrial biogenesis, and greater fatty acid oxidization in skeletal muscle (Cheol et al., 2008; Lin et al., 2002; Zhang et al., 2017). Alongside PGC-1α, several other genes, including calcineurin (CN), p38 mitogen-activated protein kinase (p38), AMP-activated protein kinase (AMPK), are key mediators of the skeletal muscle phenotype (Ljubicic et al., 2014).

2. Skeletal muscle atrophy

2.1: Introduction to skeletal muscle atrophy

Skeletal muscle atrophy is the loss of muscle mass and contractile function that results in a reduction in strength. Muscular atrophy can be caused by genetic disorders such as Duchenne muscular dystrophy (Duan et al., 2021), or acquired conditions such as cancer cachexia (Argilés et al., 2014), corticosteroid use (Bodine & Furlow, 2015), and many other chronic illnesses (Allen et al., 2016; Barreiro & Jaitovich, 2018). Regardless of the etiology, skeletal muscle atrophy is associated with an increased risk of morbidity and mortality, as well as a reduced quality of life (Chang et al., 2018; Kress & Hall, 2014; Pedersen & Saltin, 2015; Schols et al., 2005). Currently, the treatment for muscle atrophy includes nutritional supplementation and exercise as no effective pharmacological treatment exists to prevent muscle wasting (Furrer & Handschin, 2019).

Muscle fibres are unique cell types because the cytoplasm is filled with contractile proteins that are tightly surrounded by organelles like mitochondria and myonuclei. Therefore the volume or size of a muscle fibre is highly dependent on the quantity and function of these proteins (Sartori et al., 2021). In conditions of atrophy, there is a net decrease in proteins in muscle fibres that results in the shrinkage of these cells. Conversely, in response to anabolic stimuli, such as resistance exercise (Phillips et al., 1997), fibre size grows due to an increase in newly formed proteins. Therefore, the balance between protein synthesis and protein breakdown defines muscle fibre size, measured as cross-sectional area (CSA). Yet, it is becoming evident that the cellular processes and signalling pathways that regulate protein turnover within skeletal muscle are interconnected. For instance, while

exercise promotes the synthesis of new proteins, it simultaneously increases the degradation of dysfunctional organelles via autophagy (Grumati et al., 2011). The mammalian target of rapamycin complex 1 (mTORC1) signaling axis, known for initiating protein synthesis, is also activated in denervation-induced muscle atrophy (Castets et al., 2019). In fact, recent work demonstrates that hyperactivation of mTORC1 initiates proteolysis during catabolic conditions (Kaiser et al., 2022). However, the above studies were conducted in rodent models and given the discrepancy that exists in the regulation of skeletal muscle protein turnover between rodents and humans, it is unclear whether these novel findings translate to the human population (Phillips et al., 2009). Therefore, investigating the processes that mediate protein turnover (discussed in more depth in sections 2.3 and 2.4) in skeletal muscle is critical to our understanding of atrophy and for the development of targeted therapies under muscle-wasting conditions.

The various catabolic conditions evoke similar mechanisms to induce muscle atrophy, however, some differences also exist. Lecker et al. were the first to identify a common set of genes, termed atrogenes, that are differentially expressed across four conditions of atrophy: fasting, diabetes, uremia, and cancer cachexia (Lecker et al., 2004). A follow-up study demonstrated that ~80% of the previously identified atrogenes are also differentially expressed in muscle 3-days post-denervation (Sacheck et al., 2007). Among these atrogenes are those involved in the initiation of the ubiquitin-proteasome system (Mitch & Goldberg, 1996) and autophagy (Zhao et al., 2007). However, the induction of the molecular atrophy program varies across the conditions. Despite the significant overlap in the expression of atrogenes between denervation, unloading, and fasting, the expression

of the forkhead box O (FOXO) transcription factors varied significantly (Brocca et al., 2017). Additionally, fibre type-specific atrophy varies between catabolic stimuli. Systemic conditions such as cachexia and fasting, often target type II fibres, whereas in disuse-induced or neurogenic atrophy type I fibres atrophy preferentially (Ciciliot et al., 2013). The remainder of the review will focus on neurogenic muscle atrophy and its contributing cellular processes while appreciating that significant overlap exists.

2.2: Neurogenic muscle atrophy

Neurogenic muscle atrophy, also known as denervation-induced atrophy, is a form of muscle wasting caused by direct damage to the peripheral nervous system. In humans, neurogenic atrophy occurs as a response to an injury (e.g. spinal cord injury) or diseases (e.g. amyotrophic lateral sclerosis (ALS)) (Ehmsen & Höke, 2020). In mice, we can model neurogenic atrophy through nerve dissection or crush, most commonly of the sciatic nerve (Sacheck et al., 2007). Denervation of the sciatic nerve elicits more severe muscle loss than other models of disuse such as hindlimb suspension and immobilization (Bodine et al., 2001). The elimination of neuronal activity travelling to the muscle fibre inhibits its ability to contract and ultimately causes atrophic, angular fibres (Ehmsen & Höke, 2020). Early work demonstrates that the loss of muscle mass following nerve sectioning is directly proportional to the increase in protein breakdown (Goldberg, 1969), however, recent research highlights that denervation-induced proteolysis is accompanied by a decline in protein synthesis (Kobak et al., 2021). Additionally, denervation has distinctive effects across different muscles. For example, the SOL atrophies more quickly, and to a greater extent than the GAST at 3 and 7 days post-nerve section (Stouth et al., 2018, 2020). This

discrepancy could be explained by the differential response to denervation between type I and II fibres since type I fibres experience more robust atrophy (Ciciliot et al., 2013; Ehmsen & Höke, 2020). Additionally, after 50 days of denervation there is a dramatic shift to a faster, more glycolytic phenotype in both the SOL and extensor digitorm longus (EDL), a predominantly fast-twitch muscle (Patterson et al., 2006). Similarly, spinal cord injuries in humans often lead to a complete disappearance of type I fibres (Ciciliot et al., 2013). Collectively, these data indicate the severe impact of short and long-term denervation on fibre type-specific atrophy.

The drastic changes that occur in response to denervation in muscle fibres are accompanied by alterations in other cell types. An elegant study by Borisov et al. demonstrates the substantial remodeling of the microvascular network over 18 months following nerve dissection in rats (Borisov et al., 2000). They observed a linear decrease in capillary-fibre ratio over 12 months and development of significant perivascular fibrosis that contributed to the devascularization of the muscle fibres such that after 18 months, over 40% of fibres were completely avascular (Borisov et al., 2000). Moreover, muscle stem cells, termed satellite cells, have the capacity to proliferate and differentiate into myotubes in response to injury, yet their role in neurogenic atrophy remains unclear. Recent work showed that satellite cell content was unchanged in muscles 3-, 7-, and 15-days following denervation (Madaro et al., 2018). However, previous studies demonstrated an increase in satellite cell content in the early weeks post-denervation, followed by a steady decline in chronically denervated muscle (Borisov et al., 2005; W. Liu et al., 2015; Viguie et al., 1997). Interestingly, when satellite cells are genetically depleted in muscle, it

exacerbates denervation-induced atrophy (W. Liu et al., 2015). These data highlight that neurogenic atrophy induces changes in different cell types that are detrimental to skeletal muscle fibres. Several local and systemic processes and signalling networks govern the responses in muscle and non-muscle cells to muscle atrophy.

2.3: Ubiquitin-proteasome system

The ubiquitin-proteasome system is a well-established, multi-step process that regulates protein breakdown. The polyubiquitination of a target protein allows it to be recognized by the 26S proteasome and subsequently degraded (Dantuma & Bott, 2014). It was established that activation of the ubiquitin-proteasome system results in the degradation of proteins in denervated muscle (Medina et al., 1995; Wing et al., 1995). In the following years, two ubiquitin ligases were identified that regulate muscle atrophy, muscle atrophy F-box (MAFbx) and muscle RING finger 1 (MuRF1) (Bodine et al., 2001). MuRF1 and MAFbx are elevated in skeletal muscle during various catabolic conditions and have been extensively studied since their discovery (Bodine & Baehr, 2014). MuRF1 ubiquitinates several contractile proteins including myosin heavy chains and troponin, whereas MAFbx catalyzes the degradation of proteins involved in protein synthesis (Cohen et al., 2014). The genetic knockout of each of these ligases partially attenuates the loss of skeletal muscle mass 14 days following denervation in mice (Bodine et al., 2001). Transcription factors, FOXO1 and FOXO3 regulate the expression of various atrogenes, including MuRF1 and MAFbx. Muscle-specific knockout of FOXOs prevents the denervation-induced increase in MuRF1 and MAFbx and mitigates skeletal muscle atrophy (Milan et al., 2015). Additionally, in muscle biopsies from patients with ALS, MAFbx

protein and mRNA content are significantly increased, however, MuRF1 expression was unchanged (Léger et al., 2006). The importance of the ubiquitin-proteasome system in neurogenic atrophy is evident, however, additional cellular mechanisms function synergistically to contribute to skeletal muscle atrophy.

2.4: Autophagy-lysosome system

Autophagy is the other major proteolytic system that is activated during skeletal muscle atrophy (Sandri, 2013). During the process of autophagy, proteins, organelles and/or other macromolecules, are engulfed into the autophagosome and delivered to the lysosome where they are degraded (Klionsky et al., 2021). Briefly, unc-51-like kinase (ULK) is activated by the suppression of mTORC1 or by the activation of AMPK to initiate autophagosome formation (J. Kim et al., 2011). The maturation of the autophagosome involves the conversion of microtubule-associated protein 1A/1B-light chain 3 (LC3-I) into LC3-II. Proteins such as sequestosome 1 (p62), flag structures that need to be degraded and the mature autophagosome carries that cellular cargo to the lysosome where it fuses and degrades the intravesicular contents (Mulcahy Levy & Thorburn, 2020). Autophagy is required for the healthy functioning of the cell as it removes damaged or dysfunctional cellular components. In fact, it is a necessary process for the preservation of skeletal muscle mass and quality (Masiero et al., 2009). Although in catabolic conditions, the autophagy-lysosome system is hyperactivated (Deval et al., 2001; Tassa et al., 2003). A seminal study by Zhao et al. demonstrated that FOXO3 initiates protein degradation through the ubiquitin-proteasome, as well as, autophagy-lysosome systems (Zhao et al., 2007). The autophagy-lysosomal system is thought to be primarily responsible for the degradation of organelles

and sarcoplasmic proteins, whereas the ubiquitin-proteolysis targets contractile proteins (Cohen et al., 2014; Ehmsen & Höke, 2020). Denervation-induced turnover of mitochondria is attributed to enhanced degradation of the mitochondria via autophagy (i.e., mitophagy) and blunted organelle biogenesis (O'Leary et al., 2012; Triolo et al., 2022). The hyperactivation of autophagy during neurogenic atrophy may be important for the maintenance of skeletal muscle health during catabolic conditions, but additional research is needed to further elucidate its role.

3. CARM1 in skeletal muscle

3.1: Protein arginine methyltransferases

Protein arginine methyltransferases (PRMTs), are a family of enzymes that catalyze the methylation of target proteins (Bedford & Clarke, 2009; Guccione & Richard, 2019; Yang & Bedford, 2013). Specifically, PRMTs employ S-adenosylmethionine (SAM) as a methyl donor and initiate the transfer of methyl groups onto guanidine nitrogen atoms of arginine residues of proteins to produce monomethylarginine (MMA) marks. The subsequent generation of asymmetric dimethylarginine (ADMA) and symmetric dimethylarginine (SDMA) is catalyzed by type I and type II PRMTs respectively (Bedford & Clarke, 2009). PRMT1 – 4, PRMT6, and PRMT8 are type I PRMTs, whereas PRMT5 and 9 are classified as type II PRMTs. The methylation of target proteins affects their activity, localization, and/or stability and ultimately regulates cellular processes such as gene expression, mRNA splicing, and cell cycle progression (Guccione & Richard, 2019). Notably, although there is 20-50% structural homology in the amino acid sequence of the

PRMT family (Frankel et al., 2002), each enzyme has unique characteristics and localization that influence its methylation activity. For instance, PRMT3 is located exclusively in the cytosol and has a small number of targets (Frankel & Clarke, 2000), whereas PRMT1 has a wider range of substrate specificity and is responsible for approximately 85% of protein arginine methylation activity in mammalian cells (Tang et al., 2000). However, there is some redundancy between the methyltransferase function of these enzymes. When PRMT1 is genetically knocked out of cells, there is a compensatory increase in MMA marks, highlighting the substrate scavenging capacity amongst the PRMT family (Dhar et al., 2013). These enzymes are critical to cell biology, thus further research exploring their function is warranted.

3.2: The importance of CARM1

CARM1, also known as PRMT4, belongs to the PRMT family of enzymes. As its name suggests, CARM1 was first identified as a transcriptional co-activator in a genetic screening of a mouse embryo, where it was noted to have homology with a previously discovered family of enzymes, PRMTs (D. Chen et al., 1999). CARM1 regulates transcription activation by methylating histone proteins, H3R17, H3R26, and H3R42, and non-histone proteins such as transcription factors and other co-activators (Guccione & Richard, 2019; Stallcup et al., 2003; Yang & Bedford, 2013). CARM1 is expressed ubiquitously throughout the body and is indispensable to cell development (Suresh et al., 2021). In fact, the whole-body genetic knockout (KO) of CARM1 in mice results in perinatal lethality due to breathing failure (Yadav et al., 2003). These CARM1 KO mice are smaller than their wildtype littermates and display phenotypes that indicate impaired

development including decreased chondrocyte proliferation and reduced adipocyte differentiation (Ito et al., 2009; Yadav et al., 2003, 2008). Importantly, CARM1 enzyme-dead knock-in mutant mice display the same phenotype, indicating that the methyltransferase function of CARM1 is essential to its role in embryonic development (D. Kim et al., 2010). Moreover, CARM1 has unique substrate specificity from other PRMTs as it prefers methylating within proline-glycine-methionine and proline-rich motifs (Cheng et al., 2007; Shishkova et al., 2017). There are currently 26 known and validated CARM1 substrates that regulate various cellular processes, including SWI/SNF chromatin remodeling complex BAF155 (BAF155) and poly(A)-binding protein 1 (PABP1) (Suresh et al., 2021). Recently, several studies have highlighted new roles of CARM1 in cellular biology such as mediating autophagy (Suresh et al., 2021). Given that autophagy is a critical mechanism involved in skeletal muscle atrophy, investigations into the role of CARM1 in skeletal muscle are needed.

3.3: CARM1 in skeletal muscle biology

CARM1 is emerging as a regulator of skeletal muscle biology. The first study to investigate CARM1 biology in muscle demonstrated that CARM1 is necessary for differentiation as a transcriptional co-activator for myocyte enhancer factor-2C (MEF-2C) in C2C12 cells (S. L. Chen et al., 2002). Subsequent cell culture experiments demonstrated that CARM1 is also important for later stages of myogenesis through its role in mediating the transcription of myogenin (Dacwag et al., 2009). Since then, *in vivo* studies have also shown the importance of CARM1 in regeneration (Blanc & Richard, 2017; Kawabe et al., 2012). Around the same time, Ljubicic et al. found that CARM1 is elevated in dystrophic

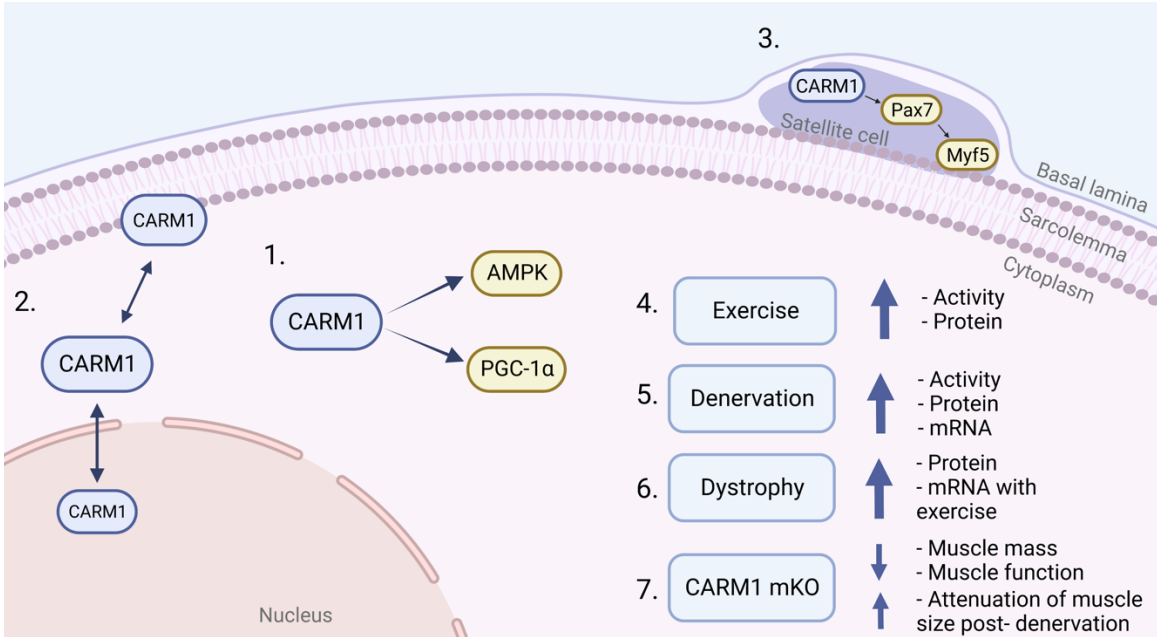

Figure 1: CARM1 biology in skeletal muscle. 1. CARM1 is present in both murine and human skeletal muscles. CARM1 interacts with important regulators of skeletal muscle biology, AMP-activated protein kinase (AMPK) and peroxisome proliferator-activated receptor-g coactivator-1α (PGC-1α). 2. CARM1 is located primarily in the cytosol but is also found at the sarcolemma and has the lowest relative subcellular expression in myonuclei. 3. CARM1 influences satellite cell activation through regulation of Myf5 via Pax7. 4. Skeletal muscle CARM1 activity increases following acute exercise in mice, and its protein content is elevated after acute and chronic exercise in humans. 5. Denervation-induced atrophy increases CARM1 enzymatic activity, mRNA levels and protein content in muscle. 6. CARM1 protein content is elevated in the skeletal muscle of dystrophic mice and exercise increases CARM1 mRNA expression. 7. Mice with a skeletal muscle-specific CARM1 knockout (CARM1 mKO) have lower muscle mass and function, however following denervation, muscle mass loss is attenuated. Adapted from vanLieshout and Ljubicic, 2019.

tissue, a catabolic condition of heightened remodeling (Ljubicic et al., 2012). Notably, CARM1 is the most abundant PRMT expressed in the skeletal muscle of humans (vanLieshout et al., 2019) and rodents (Wang et al., 2012). Recent work provides additional insight into the role of CARM1 in mediating skeletal muscle plasticity. vanLieshout et al. demonstrated that CARM1 protein content and methyltransferase activity increase following acute exercise in both human and rodent skeletal muscle (vanLieshout et al.,

2018, 2019). Furthermore, CARM1 interacts with master regulators of skeletal muscle phenotype, AMPK and peroxisome proliferator-activated receptor-γ coactivator-1α (PGC-1α) and alters AMPK-PGC-1α signal transduction (Stouth et al., 2020; vanLieshout et al., 2018). The development of skeletal muscle specific CARM1 knockout (CARM1 mKO) mice has provided additional insight into the role of CARM1 in skeletal muscle biology. CARM1 mKO mice have reduced skeletal muscle mass, CSA, and impaired grip strength compared to wildtype littermates (Stouth et al., 2020; vanLieshout et al., 2022). We recently demonstrated that in skeletal muscle protein arginine methylation occurs at the same frequency as serine and threonine phosphorylation, and lysine ubiquitination (vanLieshout et al., 2022), post-translational modifications that are well characterized in skeletal muscle phenotype plasticity (Egan & Zierath, 2013; Furrer & Handschin, 2019; Sartori et al., 2021). Additionally, CARM1 mKO mice exhibited altered transcriptomic and arginine methylproteomic signatures that characterize remodeled skeletal muscle phenotype (vanLieshout et al., 2022). Altogether, these studies highlight the importance of CARM1 in the maintenance and remodeling of skeletal muscle.

Understanding CARM1 expression and function is also of interest in the context of skeletal muscle wasting and weakness. Previous work in non-muscle cells demonstrated that CARM1 mediated the transcription and activation of autophagy-related genes (Shin et al., 2016; Yu et al., 2020). We (Stouth et al., 2018, 2020) and others (Y. Liu et al., 2019) recently found that denervation augments skeletal muscle CARM1 expression and methyltransferase activity. Interestingly, when Liu and colleagues knocked down skeletal muscle CARM1 content by ~50%, there was a preservation of muscle mass 4-weeks post-

denervation and mitigation of the molecular atrophy program (Y. Liu et al., 2019). CARM1 mKO mice also demonstrate a blunting of muscle mass and CSA loss during neurogenic disuse atrophy (Stouth et al., 2020). In both studies, the reduction or complete absence of CARM1 mitigates the activation of the ubiquitin-proteasome and autophagy-lysosome systems (Y. Liu et al., 2019; Stouth et al., 2020). These findings illustrate a potential role of CARM1 in neurogenic skeletal muscle atrophy in mice. However, the translation of these recent results to the human condition is challenging. The investigations were nonetheless timely as several small molecule PRMT inhibitor compounds are currently undergoing pre-clinical and clinical trials for various types of cancers and blood disorders (Hwang et al., 2021; Wu et al., 2021). We aim to capitalize on the recent synthesis of a robust, specific, and orally bioavailable small molecule CARM1 inhibitor compound, EZM2302 (EZM; Epizyme Inc. (Drew et al., 2017; Greenblatt et al., 2018; Mookhtiar et al., 2018)), as an additional, clinically relevant tool to explore CARM1 biology in skeletal muscle atrophy.

4. Study Objectives

The overarching purpose of this study was to characterize the effects of pharmacological CARM1 inhibition on skeletal muscle mass, function, and atrophy. The specific objectives of this thesis were to 1) determine the effectiveness of orally bio-available CARM1 inhibiting compound, EZM2302, at reducing CARM1 methyltransferase activity in skeletal muscle, 2) assess how short-term, pharmacological CARM1 inhibition affects skeletal muscle function and exercise capacity, and 3) investigate the impact of reducing CARM1 methyltransferase activity on skeletal muscle mass, CSA, and the activation of the molecular atrophy-autophagy program during neurogenic skeletal muscle atrophy. We hypothesized that the inhibition of CARM1 would modestly impair skeletal muscle function, as well as attenuate the loss of skeletal muscle mass and blunt the activation of atrophy signalling during neurogenic skeletal muscle disuse atrophy.

References:

Allen, M. D., Doherty, T. J., Rice, C. L., & Kimpinski, K. (2016). Physiology in Medicine: Neuromuscular consequences of diabetic neuropathy. In *Journal of Applied Physiology*. https://doi.org/10.1152/japplphysiol.00733.2015

Argilés, J. M., Busquets, S., Stemmler, B., & López-Soriano, F. J. (2014). Cancer cachexia: Understanding the molecular basis. In *Nature Reviews Cancer*. https://doi.org/10.1038/nrc3829

Bagshaw, C. R. (1993). *Muscle Contraction*. Springer Science & Business Media.

Barreiro, E., & Jaitovich, A. (2018). Muscle atrophy in chronic obstructive pulmonary disease: Molecular basis and potential therapeutic targets. In *Journal of Thoracic Disease*. https://doi.org/10.21037/jtd.2018.04.168

Baskin, K. K., Winders, B. R., & Olson, E. N. (2015). Muscle as a "mediator" of systemic metabolism. In *Cell Metabolism*. https://doi.org/10.1016/j.cmet.2014.12.021

Bedford, M. T., & Clarke, S. G. (2009). Protein Arginine Methylation in Mammals: Who, What, and Why. In *Molecular Cell*. https://doi.org/10.1016/j.molcel.2008.12.013

Blaauw, B., Schiaffino, S., & Reggiani, C. (2013). Mechanisms modulating skeletal muscle phenotype. *Comprehensive Physiology*. https://doi.org/10.1002/cphy.c130009

Blanc, R. S., & Richard, S. (2017). Regenerating muscle with arginine methylation. In *Transcription*. https://doi.org/10.1080/21541264.2017.1291083

Block, B. A., Imagawa, T., Campbell, K. P., & Franzini-Armstrong, C. (1988). Structural evidence for direct interaction between the molecular components of the transverse tubule/sarcoplasmic reticulum junction in skeletal muscle. *Journal of Cell Biology*. https://doi.org/10.1083/jcb.107.6.2587

Bloemberg, D., & Quadrilatero, J. (2012). Rapid determination of myosin heavy chain expression in rat, mouse, and human skeletal muscle using multicolor immunofluorescence analysis. *PLoS ONE*. https://doi.org/10.1371/journal.pone.0035273

Bodine, S. C., & Baehr, L. M. (2014). Skeletal muscle atrophy and the E3 ubiquitin ligases MuRF1 and MAFbx/atrogin-1. In *American Journal of Physiology - Endocrinology and Metabolism*. https://doi.org/10.1152/ajpendo.00204.2014

Bodine, S. C., & Furlow, J. D. (2015). Glucocorticoids and skeletal muscle. *Advances in Experimental Medicine and Biology*. https://doi.org/10.1007/978-1-4939-2895-8_7

Bodine, S. C., Latres, E., Baumhueter, S., Lai, V. K. M., Nunez, L., Clarke, B. A., Poueymirou, W. T., Panaro, F. J., Na, E., Dharmarajan, K., Pan, Z. Q., Valenzuela, D. M., Dechiara, T. M., Stitt, T. N., Yancopoulos, G. D., & Glass, D. J. (2001). Identification of ubiquitin ligases required for skeletal Muscle Atrophy. *Science*. https://doi.org/10.1126/science.1065874

Borisov, A. B., Dedkov, E. I., & Carlson, B. M. (2005). Abortive myogenesis in denervated skeletal muscle: Differentiative properties of satellite cells, their migration, and block of terminal differentiation. *Anatomy and Embryology*. https://doi.org/10.1007/s00429-004-0429-7

Borisov, A. B., Huang, S. K., & Carlson, B. M. (2000). Remodeling of the vascular bed and progressive loss of capillaries in denervated skeletal muscle. *Anatomical Record*. https://doi.org/10.1002/(SICI)1097-0185(20000301)258:3<292::AID-AR9>3.0.CO;2-N

Brocca, L., Toniolo, L., Reggiani, C., Bottinelli, R., Sandri, M., & Pellegrino, M. A. (2017). FoxO-dependent atrogenes vary among catabolic conditions and play a key role in muscle atrophy induced by hindlimb suspension. *Journal of Physiology*. https://doi.org/10.1113/JP273097

Cadot, B., Gache, V., & Gomes, E. R. (2015). Moving and positioning the nucleus in skeletal muscle-one step at a time. In *Nucleus*. https://doi.org/10.1080/19491034.2015.1090073

Castets, P., Rion, N., Théodore, M., Falcetta, D., Lin, S., Reischl, M., Wild, F., Guérard, L., Eickhorst, C., Brockhoff, M., Guridi, M., Ibebunjo, C., Cruz, J., Sinnreich, M., Rudolf, R., Glass, D. J., & Rüegg, M. A. (2019). mTORC1 and PKB/Akt control the muscle response to denervation by regulating autophagy and HDAC4. *Nature Communications*. https://doi.org/10.1038/s41467-019-11227-4

Chang, K. V., Chen, J. De, Wu, W. T., Huang, K. C., Hsu, C. T., & Han, D. S. (2018). Association between Loss of Skeletal Muscle Mass and Mortality and Tumor Recurrence in Hepatocellular Carcinoma: A Systematic Review and Meta-Analysis. In *Liver Cancer*. https://doi.org/10.1159/000484950

Chen, D., Ma, M., Hong, H., Koh, S. S., Huang, S. M., Schurter, B. T., Aswad, D. W., & Stallcup, M. R. (1999). Regulation of transcription by a protein methyltransferase. *Science*. https://doi.org/10.1126/science.284.5423.2174

Chen, S. L., Loffler, K. A., Chen, D., Stallcup, M. R., & Muscat, G. E. O. (2002). The coactivator-associated arginine methyltransferase is necessary for muscle differentiation: CARM1 coactivates myocyte enhancer factor-2. *Journal of Biological Chemistry*. https://doi.org/10.1074/jbc.M109835200

Cheng, D., Côté, J., Shaaban, S., & Bedford, M. T. (2007). The Arginine Methyltransferase CARM1 Regulates the Coupling of Transcription and mRNA Processing. *Molecular Cell*. https://doi.org/10.1016/j.molcel.2006.11.019

Cheol, S. C., Befroy, D. E., Codella, R., Kim, S., Reznick, R. M., Hwang, Y. J., Liu, Z. X., Lee, H. Y., Distefano, A., Samuel, V. T., Zhang, D., Cline, G. W., Handschin, C., Lin, J., Petersen, K. F., Spiegelman, B. M., & Shulman, G. I. (2008). Paradoxical effects of increased expression of PGC-1α on muscle mitochondrial function and insulin-stimulated muscle glucose metabolism. *Proceedings of the National*

Academy of Sciences of the United States of America. https://doi.org/10.1073/pnas.0810339105

Ciciliot, S., Rossi, A. C., Dyar, K. A., Blaauw, B., & Schiaffino, S. (2013). Muscle type and fiber type specificity in muscle wasting. In *International Journal of Biochemistry and Cell Biology*. https://doi.org/10.1016/j.biocel.2013.05.016

Cohen, S., Nathan, J. A., & Goldberg, A. L. (2014). Muscle wasting in disease: Molecular mechanisms and promising therapies. In *Nature Reviews Drug Discovery*. https://doi.org/10.1038/nrd4467

Dacwag, C. S., Bedford, M. T., Sif, S., & Imbalzano, A. N. (2009). Distinct Protein Arginine Methyltransferases Promote ATP-Dependent Chromatin Remodeling Function at Different Stages of Skeletal Muscle Differentiation. *Molecular and Cellular Biology*. https://doi.org/10.1128/mcb.00742-08

Dahl, R., Larsen, S., Dohlmann, T. L., Qvortrup, K., Helge, J. W., Dela, F., & Prats, C. (2015). Three-dimensional reconstruction of the human skeletal muscle mitochondrial network as a tool to assess mitochondrial content and structural organization. *Acta Physiologica*. https://doi.org/10.1111/apha.12289

Dantuma, N. P., & Bott, L. C. (2014). The ubiquitin-proteasome system in neurodegenerative diseases: Precipitating factor, yet part of the solution. In *Frontiers in Molecular Neuroscience*. https://doi.org/10.3389/fnmol.2014.00070

Delezie, J., & Handschin, C. (2018). Endocrine crosstalk between Skeletal muscle and the brain. In *Frontiers in Neurology*. https://doi.org/10.3389/fneur.2018.00698

Deval, C., Mordier, S., Obled, C., Bechet, D., Combaret, L., Attaix, D., & Ferrara, M. (2001). Identification of cathepsin L as a differentially expressed message associated with skeletal muscle wasting. *Biochemical Journal*. https://doi.org/10.1042/0264-6021:3600143

Dhar, S., Vemulapalli, V., Patananan, A. N., Huang, G. L., Di Lorenzo, A., Richard, S., Comb, M. J., Guo, A., Clarke, S. G., & Bedford, M. T. (2013). Loss of the major type i arginine methyltransferase PRMT1 causes substrate scavenging by other PRMTs. *Scientific Reports*. https://doi.org/10.1038/srep01311

Drew, A. E., Moradei, O., Jacques, S. L., Rioux, N., Boriack-Sjodin, A. P., Allain, C., Scott, M. P., Jin, L., Raimondi, A., Handler, J. L., Ott, H. M., Kruger, R. G., McCabe, M. T., Sneeringer, C., Riera, T., Shapiro, G., Waters, N. J., Mitchell, L. H., Duncan, K. W., … Ribich, S. A. (2017). Identification of a CARM1 Inhibitor with Potent in Vitro and in Vivo Activity in Preclinical Models of Multiple Myeloma. *Scientific Reports*. https://doi.org/10.1038/s41598-017-18446-z

Duan, D., Goemans, N., Takeda, S., Mercuri, E., & Aartsma-Rus, A. (2021). Duchenne muscular dystrophy. In *Nature Reviews Disease Primers*. https://doi.org/10.1038/s41572-021-00248-3

Egan, B., & Zierath, J. R. (2013). Exercise metabolism and the molecular regulation of skeletal muscle adaptation. In *Cell Metabolism*. https://doi.org/10.1016/j.cmet.2012.12.012

Ehmsen, J. T., & Höke, A. (2020). Cellular and molecular features of neurogenic skeletal muscle atrophy. In *Experimental Neurology*. https://doi.org/10.1016/j.expneurol.2020.113379

Fernandez-Marcos, P. J., & Auwerx, J. (2011). Regulation of PGC-1α, a nodal regulator of mitochondrial biogenesis. *American Journal of Clinical Nutrition*. https://doi.org/10.3945/ajcn.110.001917

Fitts, R. H. (2008). The cross-bridge cycle and skeletal muscle fatigue. In *Journal of Applied Physiology*. https://doi.org/10.1152/japplphysiol.01200.2007

Frankel, A., & Clarke, S. (2000). PRMT3 is a distinct member of the protein arginine N-methyltransferase family: Conferral of substrate specificity by a zinc-finger domain.

Journal of Biological Chemistry. https://doi.org/10.1074/jbc.M006445200

Frankel, A., Yadav, N., Lee, J., Branscombe, T. L., Clarke, S., & Bedford, M. T. (2002). The novel human protein arginine N-methyltransferase PRMT6 is a nuclear enzyme displaying unique substrate specificity. *Journal of Biological Chemistry*. https://doi.org/10.1074/jbc.M108786200

Frontera, W. R., & Ochala, J. (2015). Skeletal Muscle: A Brief Review of Structure and Function. In *Behavior Genetics*. https://doi.org/10.1007/s00223-014-9915-y

Furrer, R., & Handschin, C. (2019). Muscle wasting diseases: Novel targets and treatments. In *Annual Review of Pharmacology and Toxicology*. https://doi.org/10.1146/annurev-pharmtox-010818-021041

Goldberg, A. L. (1969). Protein turnover in skeletal muscle. II. Effects of denervation and cortisone on protein catabolism in skeletal muscle. *Journal of Biological Chemistry*.

Greenblatt, S. M., Man, N., Hamard, P. J., Asai, T., Karl, D., Martinez, C., Bilbao, D., Stathais, V., McGrew-Jermacowicz, A., Duffort, S., Tadi, M., Blumenthal, E., Newman, S., Vu, L., Xu, Y., Liu, F., Schurer, S. C., McCabe, M. T., Kruger, R. G., … Nimer, S. D. (2018). CARM1 Is Essential for Myeloid Leukemogenesis but Dispensable for Normal Hematopoiesis. *Cancer Cell*. https://doi.org/10.1016/j.ccell.2018.05.007

Grumati, P., Coletto, L., Schiavinato, A., Castagnaro, S., Bertaggia, E., Sandri, M., & Bonaldo, P. (2011). Physical exercise stimulates autophagy in normal skeletal muscles but is detrimental for collagen VI-deficient muscles. *Autophagy*. https://doi.org/10.4161/auto.7.12.17877

Guccione, E., & Richard, S. (2019). The regulation, functions and clinical relevance of arginine methylation. In *Nature Reviews Molecular Cell Biology*. https://doi.org/10.1038/s41580-019-0155-x

Hwang, J. W., Cho, Y., Bae, G. U., Kim, S. N., & Kim, Y. K. (2021). Protein arginine methyltransferases: promising targets for cancer therapy. In *Experimental and Molecular Medicine*. https://doi.org/10.1038/s12276-021-00613-y

Ito, T., Yadav, N., Lee, J., Furumatsu, T., Yamashita, S., Yoshida, K., Taniguchi, N., Hashimoto, M., Tsuchiya, M., Ozaki, T., Lotz, M., Bedford, M. T., & Asahara, H. (2009). Arginine methyltransferase CARM1/PRMT4 regulates endochondral ossification. *BMC Developmental Biology*. https://doi.org/10.1186/1471-213X-9-47

Kaiser, M. S., Milan, G., Ham, D. J., Lin, S., Oliveri, F., Chojnowska, K., ... & Rüegg, M. A. (2022). Dual roles of mTORC1-dependent activation of the ubiquitin-proteasome system in muscle proteostasis. *Communications biology*, *5*(1), 1-18.

Kalyani, R. R., Corriere, M., & Ferrucci, L. (2014). Age-related and disease-related muscle loss: The effect of diabetes, obesity, and other diseases. In *The Lancet Diabetes and Endocrinology*. https://doi.org/10.1016/S2213-8587(14)70034-8

Kawabe, Y. I., Wang, Y. X., McKinnell, I. W., Bedford, M. T., & Rudnicki, M. A. (2012). Carm1 regulates Pax7 transcriptional activity through MLL1/2 recruitment during asymmetric satellite stem cell divisions. *Cell Stem Cell*. https://doi.org/10.1016/j.stem.2012.07.001

Kim, D., Lee, J., Cheng, D., Li, J., Carter, C., Richie, E., & Bedford, M. T. (2010). Enzymatic activity is required for the in Vivo functions of CARM1. *Journal of Biological Chemistry*. https://doi.org/10.1074/jbc.M109.035865

Kim, J., Kundu, M., Viollet, B., & Guan, K. L. (2011). AMPK and mTOR regulate autophagy through direct phosphorylation of Ulk1. *Nature Cell Biology*. https://doi.org/10.1038/ncb2152

Klionsky, D. J., Petroni, G., Amaravadi, R. K., Baehrecke, E. H., Ballabio, A., Boya, P., Bravo-San Pedro, J. M., Cadwell, K., Cecconi, F., Choi, A. M. K., Choi, M. E., Chu, C. T., Codogno, P., Colombo, M. I., Cuervo, A. M., Deretic, V., Dikic, I., Elazar, Z., Eskelinen, E., … Pietrocola, F. (2021). Autophagy in major human diseases. *The*

EMBO Journal. https://doi.org/10.15252/embj.2021108863

Kobak, K. A., Lawrence, M. M., Pharaoh, G., Borowik, A. K., Peelor, F. F., Shipman, P. D., Griffin, T. M., Van Remmen, H., & Miller, B. F. (2021). Determining the contributions of protein synthesis and breakdown to muscle atrophy requires non-steady-state equations. *Journal of Cachexia, Sarcopenia and Muscle*. https://doi.org/10.1002/jcsm.12772

Kress, J. P., & Hall, J. B. (2014). ICU-Acquired Weakness and Recovery from Critical Illness. *New England Journal of Medicine*. https://doi.org/10.1056/nejmra1209390

Lecker, S. H., Jagoe, R. T., Gilbert, A., Gomes, M., Baracos, V., Bailey, J., Price, S. R., Mitch, W. E., & Goldberg, A. L. (2004). Multiple types of skeletal muscle atrophy involve a common program of changes in gene expression. *The FASEB Journal*. https://doi.org/10.1096/fj.03-0610com

Léger, B., Vergani, L., Sorarù, G., Hespel, P., Derave, W., Gobelet, C., D'Ascenzio, C., Angelini, C., & Russell, A. P. (2006). Human skeletal muscle atrophy in amyotrophic lateral sclerosis reveals a reduction in Akt and an increase in atrogin-1. *The FASEB Journal*. https://doi.org/10.1096/fj.05-5249fje

Lin, J., Wu, H., Tarr, P. T., Zhang, C. Y., Wu, Z., Boss, O., Michael, L. F., Puigserver, P., Isotani, E., Olson, E. N., Lowell, B. B., Bassel-Duby, R., & Spiegelman, B. M. (2002). Transcriptional co-activator PGC-1α drives the formation of slow-twitch muscle fibres. *Nature*. https://doi.org/10.1038/nature00904

Liu, W., Wei-LaPierre, L., Klose, A., Dirksen, R. T., & Chakkalakal, J. V. (2015). Inducible depletion of adult skeletal muscle stem cells impairs the regeneration of neuromuscular junctions. *ELife*. https://doi.org/10.7554/eLife.09221

Liu, Y., Li, J., Shang, Y., Guo, Y., & Li, Z. (2019). CARM1 contributes to skeletal muscle wasting by mediating FoxO3 activity and promoting myofiber autophagy. *Experimental Cell Research*. https://doi.org/10.1016/j.yexcr.2018.11.024

Ljubicic, V., Burt, M., & Jasmin, B. J. (2014). The therapeutic potential of skeletal muscle plasticity in Duchenne muscular dystrophy: Phenotypic modifiers as pharmacologic targets. In *FASEB Journal*. https://doi.org/10.1096/fj.13-238071

Ljubicic, V., Khogali, S., Renaud, J. M., & Jasmin, B. J. (2012). Chronic AMPK stimulation attenuates adaptive signaling in dystrophic skeletal muscle. *American Journal of Physiology - Cell Physiology*. https://doi.org/10.1152/ajpcell.00183.2011

Madaro, L., Passafaro, M., Sala, D., Etxaniz, U., Lugarini, F., Proietti, D., Alfonsi, M. V., Nicoletti, C., Gatto, S., De Bardi, M., Rojas-García, R., Giordani, L., Marinelli, S., Pagliarini, V., Sette, C., Sacco, A., & Puri, P. L. (2018). Denervation-activated STAT3–IL-6 signalling in fibro-adipogenic progenitors promotes myofibres atrophy and fibrosis. *Nature Cell Biology*. https://doi.org/10.1038/s41556-018-0151-y

Masiero, E., Agatea, L., Mammucari, C., Blaauw, B., Loro, E., Komatsu, M., Metzger, D., Reggiani, C., Schiaffino, S., & Sandri, M. (2009). Autophagy Is Required to Maintain Muscle Mass. *Cell Metabolism*. https://doi.org/10.1016/j.cmet.2009.10.008

Mauro, A. (1961). Satellite cell of skeletal muscle fibers. *The Journal of Biophysical and Biochemical Cytology*. https://doi.org/10.1083/jcb.9.2.493

Medina, R., Wing, S. S., & Goldberg, A. L. (1995). Increase in levels of polyubiquitin and proteasome mRNA in skeletal muscle during starvation and denervation atrophy. *Biochemical Journal*. https://doi.org/10.1042/bj3070631

Milan, G., Romanello, V., Pescatore, F., Armani, A., Paik, J. H., Frasson, L., Seydel, A., Zhao, J., Abraham, R., Goldberg, A. L., Blaauw, B., DePinho, R. A., & Sandri, M. (2015). Regulation of autophagy and the ubiquitin-proteasome system by the FoxO transcriptional network during muscle atrophy. *Nature Communications*. https://doi.org/10.1038/ncomms7670

Mitch, W. E., & Goldberg, A. L. (1996). Mechanisms of Muscle Wasting — The Role of the Ubiquitin–Proteasome Pathway. *New England Journal of Medicine*. https://doi.org/10.1056/nejm199612193352507

Mookhtiar, A. K., Greenblatt, S., Man, N., Karl, D., Stathias, V., Schurer, S., & Nimer, S. D. (2018). CARM1 Inhibition: Evaluation of Response and Efficacy in Acute Myeloid Leukemia. *Blood*. https://doi.org/10.1182/blood-2018-99-114981

Mulcahy Levy, J. M., & Thorburn, A. (2020). Autophagy in cancer: moving from understanding mechanism to improving therapy responses in patients. In *Cell Death and Differentiation*. https://doi.org/10.1038/s41418-019-0474-7

O'Leary, M. F. N., Vainshtein, A., Carter, H. N., Zhang, Y., & Hood, D. A. (2012). Denervation-induced mitochondrial dysfunction and autophagy in skeletal muscle of apoptosis-deficient animals. *American Journal of Physiology - Cell Physiology*. https://doi.org/10.1152/ajpcell.00451.2011

Patterson, M. F., Stephenson, G. M. M., & Stephenson, D. G. (2006). Denervation produces different single fiber phenotypes in fast- and slow-twitch hindlimb muscles of the rat. *American Journal of Physiology - Cell Physiology*. https://doi.org/10.1152/ajpcell.00013.2006

Pedersen, B. K., & Saltin, B. (2015). Exercise as medicine - Evidence for prescribing exercise as therapy in 26 different chronic diseases. *Scandinavian Journal of Medicine and Science in Sports*. https://doi.org/10.1111/sms.12581

Phillips, S. M., Glover, E. I., & Rennie, M. J. (2009). Alterations of protein turnover underlying disuse atrophy in human skeletal muscle. In *Journal of Applied Physiology*. https://doi.org/10.1152/japplphysiol.00452.2009

Phillips, S. M., Tipton, K. D., Aarsland, A., Wolf, S. E., & Wolfe, R. R. (1997). Mixed muscle protein synthesis and breakdown after resistance exercise in humans. *American Journal of Physiology - Endocrinology and Metabolism*. https://doi.org/10.1152/ajpendo.1997.273.1.e99

Purslow, P. P. (2020). The Structure and Role of Intramuscular Connective Tissue in Muscle Function. In *Frontiers in Physiology*. https://doi.org/10.3389/fphys.2020.00495

Sacheck, J. M., Hyatt, J. K., Raffaello, A., Thomas Jagoe, R., Roy, R. R., Reggie Edgerton, V., Lecker, S. H., & Goldberg, A. L. (2007). Rapid disuse and denervation atrophy involve transcriptional changes similar to those of muscle wasting during systemic diseases. *The FASEB Journal*. https://doi.org/10.1096/fj.06-6604com

Sandri, M. (2013). Protein breakdown in muscle wasting: Role of autophagy-lysosome and ubiquitin-proteasome. In *International Journal of Biochemistry and Cell Biology*. https://doi.org/10.1016/j.biocel.2013.04.023

Sartori, R., Romanello, V., & Sandri, M. (2021). Mechanisms of muscle atrophy and hypertrophy: implications in health and disease. In *Nature Communications*. https://doi.org/10.1038/s41467-020-20123-1

Schiaffino, S. (2010). Fibre types in skeletal muscle: A personal account. In *Acta Physiologica*. https://doi.org/10.1111/j.1748-1716.2010.02130.x

Schols, A. M. W. J., Broekhuizen, R., Weling-Scheepers, C. A., & Wouters, E. F. (2005). Body composition and mortality in chronic obstructive pulmonary disease. *American Journal of Clinical Nutrition*. https://doi.org/10.1093/ajcn/82.1.53

Shin, H. J. R., Kim, H., Oh, S., Lee, J. G., Kee, M., Ko, H. J., Kweon, M. N., Won, K. J., & Baek, S. H. (2016). AMPK-SKP2-CARM1 signalling cascade in transcriptional regulation of autophagy. *Nature*. https://doi.org/10.1038/nature18014

Shishkova, E., Zeng, H., Liu, F., Kwiecien, N. W., Hebert, A. S., Coon, J. J., & Xu, W. (2017). Global mapping of CARM1 substrates defines enzyme specificity and substrate recognition. *Nature Communications*. https://doi.org/10.1038/ncomms15571

Snijders, T., Nederveen, J. P., McKay, B. R., Joanisse, S., Verdijk, L. B., van Loon, L. J. C., & Parise, G. (2015). Satellite cells in human skeletal muscle plasticity. In *Frontiers in Physiology*. https://doi.org/10.3389/fphys.2015.00283

Stallcup, M. R., Kim, J. H., Teyssier, C., Lee, Y. H., Ma, H., & Chen, D. (2003). The roles of protein-protein interactions and protein methylation in transcriptional activation by nuclear receptors and their coactivators. *Journal of Steroid Biochemistry and Molecular Biology*. https://doi.org/10.1016/S0960-0760(03)00222-X

Staron, R. S., & Pette, D. (1993). The continuum of pure and hybrid myosin heavy chain-based fibre types in rat skeletal muscle. *Histochemistry*. https://doi.org/10.1007/BF00572901

Stouth, D. W., Manta, A., & Ljubicic, V. (2018). Protein arginine methyltransferase expression, localization, and activity during disuse-induced skeletal muscle plasticity. *American Journal of Physiology - Cell Physiology*. https://doi.org/10.1152/ajpcell.00174.2017

Stouth, D. W., vanLieshout, T. L., Ng, S. Y., Webb, E. K., Manta, A., Moll, Z., & Ljubicic, V. (2020). CARM1 Regulates AMPK Signaling in Skeletal Muscle. *IScience*. https://doi.org/10.1016/j.isci.2020.101755

Suresh, S., Huard, S., & Dubois, T. (2021). CARM1/PRMT4: Making Its Mark beyond Its Function as a Transcriptional Coactivator. In *Trends in Cell Biology*. https://doi.org/10.1016/j.tcb.2020.12.010

Tang, J., Frankel, A., Cook, R. J., Kim, S., Paik, W. K., Williams, K. R., Clarke, S., & Herschman, H. R. (2000). PRMT1 is the predominant type I protein arginine methyltransferase in mammalian cells. *Journal of Biological Chemistry*. https://doi.org/10.1074/jbc.275.11.7723

Tassa, A., Roux, M. P., Attaix, D., & Bechet, D. M. (2003). Class III phosphoinositide 3-kinase-Beclin1 complex mediates the amino acid-dependent regulation of autophagy in C2C12 myotubes. *Biochemical Journal*. https://doi.org/10.1042/BJ20030826

Triolo, M., Slavin, M., Moradi, N., & Hood, D. A. (2022). Time-dependent changes in autophagy, mitophagy and lysosomes in skeletal muscle during denervation-induced disuse. *Journal of Physiology*. https://doi.org/10.1113/JP282173

vanLieshout, T. L., Bonafiglia, J. T., Gurd, B. J., & Ljubicic, V. (2019). Protein arginine methyltransferase biology in humans during acute and chronic skeletal muscle plasticity. *Journal of Applied Physiology*. https://doi.org/10.1152/japplphysiol.00142.2019

vanLieshout, T. L., Stouth, D. W., Hartel, N. G., Vasam, G., Ng, S. Y., Webb, E. K., Rebalka, I. A., Mikhail, A. I., Graham, N. A., Menzies, K. J., Hawke, T. J., & Ljubicic, V. (2022). The CARM1 transcriptome and arginine methylproteome mediate skeletal muscle integrative biology. *Molecular Metabolism*, *64*(July), 101555. https://doi.org/10.1016/j.molmet.2022.101555

vanLieshout, T. L., Stouth, D. W., Tajik, T., & Ljubicic, V. (2018). Exercise-induced Protein Arginine Methyltransferase Expression in Skeletal Muscle. *Medicine and Science in Sports and Exercise*. https://doi.org/10.1249/MSS.0000000000001476

Vettor, R., Milan, G., Franzin, C., Sanna, M., De Coppi, P., Rizzuto, R., & Federspil, G. (2009). The origin of intermuscular adipose tissue and its pathophysiological implications. In *American Journal of Physiology - Endocrinology and Metabolism*. https://doi.org/10.1152/ajpendo.00229.2009

Viguie, C. A., Lu, D. A. X., Huang, S. K., Rengen, H., & Carlson, B. M. (1997). Quantitative study of the effects of long-term denervation on the extensor digitorum longus muscle of the rat. *Anatomical Record*. https://doi.org/10.1002/(SICI)1097-0185(199707)248:3<346::AID-AR7>3.0.CO;2-N

Wang, S. C. M., Dowhan, D. H., Eriksson, N. A., & Muscat, G. E. O. (2012). CARM1/PRMT4 is necessary for the glycogen gene expression programme in skeletal muscle cells. *Biochemical Journal*. https://doi.org/10.1042/BJ20112033

Wing, S. S., Haas, A. L., & Goldberg, A. L. (1995). Increase in ubiquitin-protein conjugates concomitant with the increase in proteolysis in rat skeletal muscle during starvation and atrophy denervation. *Biochemical Journal*. https://doi.org/10.1042/bj3070639

Wu, Q., Schapira, M., Arrowsmith, C. H., & Barsyte-Lovejoy, D. (2021). Protein arginine methylation: from enigmatic functions to therapeutic targeting. In *Nature Reviews Drug Discovery*. https://doi.org/10.1038/s41573-021-00159-8

Yadav, N., Cheng, D., Richard, S., Morel, M., Iyer, V. R., Aldaz, C. M., & Bedford, M. T. (2008). CARM1 promotes adipocyte differentiation by coactivating PPARγ. *EMBO Reports*. https://doi.org/10.1038/sj.embor.7401151

Yadav, N., Lee, J., Kim, J., Shen, J., Hu, M. C. T., Aldaz, C. M., & Bedford, M. T. (2003). Specific protein methylation defects and gene expression perturbations in coactivator-associated arginine methyltransferase 1-deficient mice. *Proceedings of the National Academy of Sciences of the United States of America*. https://doi.org/10.1073/pnas.1232272100

Yang, Y., & Bedford, M. T. (2013). Protein arginine methyltransferases and cancer. In *Nature Reviews Cancer*. https://doi.org/10.1038/nrc3409

Yu, Y. S., Shin, H. R., Kim, D., Baek, S. A., Choi, S. A., Ahn, H., Shamim, A., Kim, J., Kim, I. S., Kim, K. K., Won, K. J., & Baek, S. H. (2020). Pontin arginine methylation by CARM1 is crucial for epigenetic regulation of autophagy. *Nature Communications*. https://doi.org/10.1038/s41467-020-20080-9

Zhang, L., Zhou, Y., Wu, W., Hou, L., Chen, H., Zuo, B., Xiong, Y., & Yang, J. (2017). Skeletal muscle-specific overexpression of PGC-1α induces fiber-type conversion through enhanced mitochondrial respiration and fatty acid oxidation in mice and pigs. *International Journal of Biological Sciences*. https://doi.org/10.7150/ijbs.20132

Zhao, J., Brault, J. J., Schild, A., Cao, P., Sandri, M., Schiaffino, S., Lecker, S. H., & Goldberg, A. L. (2007). FoxO3 Coordinately Activates Protein Degradation by the Autophagic/Lysosomal and Proteasomal Pathways in Atrophying Muscle Cells. *Cell Metabolism*. https://doi.org/10.1016/j.cmet.2007.11.004

Zierath, J. R., & Hawley, J. A. (2004). Skeletal muscle fiber type: Influence on contractile and metabolic properties. In *PLoS Biology*. https://doi.org/10.1371/journal.pbio.0020348

Zot, A. S., & Potter, J. D. (1987). Structural aspects of troponin-tropomyosin regulation of skeletal muscle contraction. In *Annual review of biophysics and biophysical chemistry*. https://doi.org/10.1146/annurev.bb.16.060187.002535

Effects of short-term, pharmacological CARM1 inhibition on skeletal muscle mass, function, and atrophy

Erin K. Webb, Sean Y. Ng, Andrew I. Mikhail, Derek W. Stouth, Tiffany L. vanLieshout, Anika L. Syroid, and Vladimir Ljubicic

Department of Kinesiology, McMaster University, Hamilton, ON, Canada

Abstract

Coactivator-associated arginine methyltransferase 1 (CARM1) catalyzes the methylation of arginine residues on target proteins critical for health and disease. The purpose of this study was to characterize the effects of short-term, pharmacological CARM1 inhibition on skeletal muscle size, function, and atrophy. Adult mice (n = 10-11/sex) were treated with either a CARM1 inhibitor (150 mg/kg EZM2302; EZM) or vehicle (Veh) via oral gavage for 11-13 days and muscle mass, function, and exercise capacity were assessed. Additionally, we investigated the effect of CARM1 suppression on unilateral hindlimb denervation (DEN)-induced muscle atrophy (n = 8/sex). We report that CARM1 inhibition caused significant reductions in the asymmetric dimethylation of known CARM1 substrates but no change in CARM1 protein or mRNA content in skeletal muscle. Reduced CARM1 activity did not affect body or muscle mass, however, we observed a decrease in exercise capacity and muscular endurance in male mice. CARM1 methyltransferase activity increased in the muscle of Veh-treated mice following 7 days of DEN and this response was blunted in EZM-dosed mice. Skeletal muscle mass and myofiber cross-sectional area were significantly reduced in DEN compared to contralateral, non-DEN limbs to a similar degree in both treatment groups. Furthermore, skeletal muscle atrophy and autophagy gene expression programs were elevated in response to DEN independent of CARM1 suppression. Collectively, these results suggest that short-term, pharmacological CARM1 inhibition in adult animals affects muscle performance in a sex-specific manner but does not impact the maintenance and remodeling of skeletal muscle mass during conditions of neurogenic muscle atrophy.

Introduction

Coactivator-associated arginine methyltransferase 1 (CARM1) belongs to a family of enzymes known as protein arginine methyltransferases (PRMTs) that catalyze the transfer of methyl groups onto arginine residues of target proteins. Specifically, CARM1 (also known as PRMT4) catalyses the addition of a single methyl group onto a terminal nitrogen atom of an arginine to synthesize a monomethylarginine (MMA) modification and/or a second methyl group to create an asymmetric dimethylarginine (ADMA) mark. The addition of methyl groups to arginine residues on histone and non-histone proteins may modify their physical and chemical properties to ultimately alter their activity and/or subcellular localization (Bedford & Clarke, 2009; Guccione & Richard, 2019). Arginine methylation occurs in human cells at the same frequency as other better understood, post-translational modifications such as phosphorylation and ubiquitination (Larsen et al., 2016) and is required for several cellular processes (Bedford & Clarke, 2009; Guccione & Richard, 2019). In fact, the whole-body genetic deletion of CARM1 results in perinatal lethality in mice (Kim et al., 2010; Yadav et al., 2003). Moreover, in a cohort of over 141,000 participants, zero loss-of-function mutations in CARM1 were identified, which suggests that CARM1 is required for survival in humans as well (Jamet et al., 2022; Karczewski et al., 2020). Collectively, these data demonstrate that CARM1 plays critical roles in cell biology.

We recently demonstrated that in skeletal muscle, the prevalence of protein arginine methylation occurs on par with the extent of serine and threonine phosphorylation, and lysine ubiquitination (vanLieshout et al., 2022), post-translational modifications that are

much more studied and better understood to affect muscle phenotype maintenance and plasticity (Egan & Zierath, 2013; Furrer & Handschin, 2019; Sartori et al., 2021). Furthermore, we observed that CARM1 skeletal muscle-specific knockout (mKO) mice exhibited altered transcriptomic and arginine methylproteomic signatures with molecular and functional outcomes confirming remodeled skeletal muscle contractile and neuromuscular junction characteristics, which presaged decreased exercise tolerance (vanLieshout et al., 2022). Thus, CARM1 has emerged as an important regulator of skeletal muscle plasticity (vanLieshout & Ljubicic, 2019). This is not surprising since: 1) CARM1 is the most highly expressed PRMT transcript in rodent (Wang et al., 2012) and human (vanLieshout et al., 2019) skeletal muscle, and 2) CARM1 interacts with master regulators of skeletal muscle phenotype AMP-activated protein kinase (AMPK) and peroxisome proliferator-activated receptor-γ coactivator-1α (PGC-1α) (Stouth et al., 2020; vanLieshout et al., 2018) and alters the activity of the AMPK-PGC-1α signaling axis (Stouth et al., 2020; vanLieshout et al., 2022).

Given its role in skeletal muscle remodeling, regeneration, and repair (vanLieshout & Ljubicic, 2019), understanding CARM1 expression and function are of interest in the context of skeletal muscle wasting and weakness. We (Stouth et al., 2018, 2020) and others (Liu et al., 2019) have previously found that denervation (DEN) augments muscle CARM1 expression and methyltransferase activity concomitant with expected neurogenic disuse-induced muscle loss. Interestingly, in adult mice where skeletal muscle CARM1 content is transiently knocked down, as well as in CARM1 mKO animals, there is a preservation of muscle mass post-DEN and mitigation of the molecular atrophy program (Liu et al., 2019;

Stouth et al., 2020). These findings were timely, as several small molecule PRMT inhibitor compounds are currently undergoing pre-clinical and clinical trials for various types of cancers (Hwang et al., 2021; Q. Wu et al., 2021). However, the impact of pharmacological CARM1 inhibition on skeletal muscle biology is unknown. Thus, the purpose of the present study was to characterize the effects of CARM1 methyltransferase inhibition in adult mice (Drew et al., 2017; Greenblatt et al., 2018; Hwang et al., 2021; Mookhtiar et al., 2018) on skeletal muscle mass, function, and atrophy. We hypothesized that global, pharmacological CARM1 inhibition would modestly impair skeletal muscle function, as well as attenuate the loss of mass and activation of atrophic signaling during neurogenic-disuse skeletal muscle atrophy.

Methods

Animals. Young, (12-16-week-old) healthy female and male mice of C57BL6J/129 background were housed in an environmentally controlled room and provided food and water ad libitum. Following experiments, mice were euthanized via cervical dislocation and the gastrocnemius (GAST), soleus (SOL), quadriceps (QUAD), tibialis anterior (TA), triceps (TRI), and extensor digitorum longus (EDL) muscles, as well as liver, were harvested. GAST, QUAD, TA, and TRI muscles were weighed and immediately flash frozen in liquid nitrogen, while SOL and EDL muscles were weighed and mounted in optimum cutting temperature compound (OCT; Fisher Scientific; Hampton, NH, USA) and frozen in isopentane cooled in liquid nitrogen. All tissues were stored at -80 °C until

analysis. All mice were housed and cared for according to the Canadian Council on Animal Care guidelines in the McMaster Central Animal Facility.

Pharmacological inhibition of CARM1. Male and female mice were randomized into either vehicle (Veh) or EZM2302 (EZM; Epizyme, Cambridge, MA, USA) treatment groups. The Veh [0.5% sodium carboxymethyl cellulose (Sigma Aldrich; St. Louis, MO, USA) in ddH_2O] and EZM (150 mg/kg) solutions were prepared weekly and stored according to the manufacturer's suggestions (Drew et al., 2017). Mice were treated BID at 12-hour intervals via oral gavage for the duration of each study.

Evaluation of skeletal muscle function, exercise capacity, and locomotor behaviours. Male and female mice received either Veh or EZM for 11 days (n = 4-5 animals of each sex per group) or 13 days (n = 5-6 mice of each sex per group). On the 8th and 9th days of treatment, mice underwent a brief familiarization for each in vivo functional test (detailed below). On the 10th day of treatment, functional assessments were completed on all mice. The animals treated for 11 days were euthanized on the 11th day approximately 24 hours after the cessation of the final test, while the cohort of remaining mice performed a single bout of treadmill running on the 11th day to assess exercise capacity and their tissues were collected on the 13th day, approximately 48 hours after the treadmill run.

Mice underwent forelimb and all limb grip strength measurements (Aartsma-Rus & van Putten, 2014) by pulling on a grid-grip dynamometer (Columbus Instruments; Columbus, OH, USA). On the testing day, each mouse performed 3 successive pull attempts and was then returned to their cage for a rest period of 1 minute. This was repeated 5 times, for a total of 15 attempts. Maximum grip strength was determined by taking the

average of the 3 highest successive values out of the 15 pulls recorded and normalizing to body weight in grams. Fatigue was determined by calculating the decrement between the average of the first 2 series of attempts (1 + 2 + 3 = A, 4 + 5 + 6 = B) and the last 2 series of pulls (10 + 11 +12 = C, 13 + 14 + 15 = D) using formula (C + D)/(A + B).

Rotarod testing was performed to evaluate motor coordination (Aartsma-Rus & van Putten, 2014). During data collection the mouse was placed on the rotarod, which accelerated from 5 to 45 rpm over 300 seconds, followed by an additional 300 seconds at 45 rpm. The time and speed at failure were recorded. The test was performed 3 times for each animal and the best of these trials was used for statistical analysis.

The hang test examined mice for balance and muscular endurance (Aartsma-Rus & van Putten, 2014). For this test, mice were placed on a metal cage lid and once the mouse grasped the lid, it was inverted and held in the same position for the duration of the test. The time at failure was recorded. The mice performed 3 trials and the best time (i.e., longest duration before falling) of these 3 trials was used for statistical analysis. If a mouse fell off within 3 seconds of hanging from the cage, the test was restarted, and that trial was not counted.

Movement behaviour was measured using an open-field Opto-Varimex-5 Auto-Track (Columbus Instruments; Columbus, OH, USA) (Tatem et al., 2014). Mice were placed into the centre of the open-field and underwent a 1-hour data collection session in a quiet environment without disruption. A variety of activity measures were recorded, including distance travelled, average speed and resting time.

For the assessment of exercise capacity, mice were challenged with a single bout of exhaustive exercise on a motor-driven rodent treadmill (Columbus Instruments; Columbus, OH, USA). The exercise protocol began at 15 metres/minute and increased by 5 metres/minute at the 10- and 20-minute marks. The incline began at 5° and increased by 5° at the 30-, 40- and 70-minute marks. If mice could continue running beyond 90 minutes, the speed was increased by 5 metres/minute every 5 minutes until exhaustion, which was determined by the cessation of exercise despite probing with a soft bristle brush for 5 seconds (Saleem et al., 2014).

Denervation (DEN) experiments. Male and female mice received either Veh or EZM for 11 days (n = 8 animals of each sex per group). On the 5th day of treatment, unilateral sectioning of the sciatic nerve was performed. This model of neurogenic muscle atrophy evokes a rapid and robust remodelling of skeletal muscle in the DEN limb, while also allowing for use of the contralateral, innervated limb to serve as an intra-animal control (CON). Mice were subjected to 7 days of DEN, and on the 11th day, animals were euthanatized, and tissues were weighed and collected.

Surgery was performed as previously described (Stouth et al., 2018, 2020). Briefly, mice were anesthetized by isoflurane inhalation (Fresenius Kabi; Bad Homburg, HE, Germany) before surgery and continued to receive isoflurane via nose cone for the duration of the surgery. Prior to the operation, a 5 mg/kg subcutaneous injection of carprofen (Zoetis; Lincoln, NE, USA) was given subcutaneously for post-operative analgesia. A 1-2 cm skin incision was made in the posterior thigh musculature and blunt dissection was employed to expose the sciatic nerve. Unilateral DEN of the lower limb was induced by

excising a ~ 0.5 cm section of the sciatic nerve in the right hind limb. The overlying musculature was sutured with silk (Ethicon Inc.; Somerville, NJ, USA), and the skin was secured using veterinary staples (Mikron Precision Inc.; Gardena, CA, USA). The mice recovered in their cage on a heating pad and were weighed and monitored daily.

Protein extraction and quantification. A portion of frozen GAST muscle (~30 mg) was mechanically crushed with a tissue pulverizer (Cellcrusher; Cork, Ireland) in a liquid nitrogen bath and placed in RIPA buffer (Sigma Aldrich; 20 mL of RIPA per 1 mg muscle weight) supplemented with a protease and phosphatase inhibitor cocktail (Roche; Laval, QC, Canada). 1 stainless steel ball was added into each sample tube and then loaded into a pre-cooled Tissue Lyser (Qiagen; Toronto, ON, Canada) and run for 5 bouts of 30 seconds at a frequency of 20.0 1/second. The ball was then removed using clean tweezers and samples were sonicated for 5 x 5 seconds at maximum power. Following this, samples were spun in a centrifuge at 14,000 g for 10 minutes at 4 °C. The resulting supernates were then collected and a bicinchoninic assay (BCA; Thermofisher Scientific, Toronto, ON, Canada) was performed to determine protein concentration. All samples were diluted with 4X loading buffer and ultra-pure water to a final concentration of 2 μg/μL.

Western blotting. Samples (20 μg) were separated on a 4-20% Criterion TGX precast protein gel (Bio-Rad Laboratories; Mississauga, ON, Canada) for 55 minutes at 200 V. Afterwards, proteins were transferred onto nitrocellulose membranes using a Trans-Blot Turbo transfer system (Bio-Rad Laboratories). Subsequently, a Stain-Free image of the membrane was obtained using ChemiDoc MP Imaging System (Bio-Rad Laboratories) to verify equal sample loading. Membranes were placed in blocking solution [5% BSA in 1X

Tris-buffered saline with 1% Tween-20 (TBST)] for 1 hour at room temperature, then incubated overnight at 4 °C with primary antibodies. Blots were then washed in 1X TBST for 3 x 5 minutes and incubated in the appropriate secondary antibody for 75 minutes at room temperature. Next, membranes were washed in 1X TBST buffer for 3 x 5 minutes again prior to applying luminol-based enhanced chemiluminescence reagent (Bio-Rad Laboratories) for visualization. Finally, membranes were imaged using ChemiDoc MP Imaging System and densitometry was performed on Image Lab software (Bio-Rad Laboratories).

The following primary antibodies were used: CARM1 (1:5,000; A300-421A; Bethyl Laboratories; Montgomery, TX, USA), ADMA)-marked CARM1 substrates [CARM1 substrates; 1:1,000; a kind gift from Dr. Mark Bedford, MD Anderson Cancer Center, University of Texas (D. Cheng et al., 2018)], ADMA-marked SWI/SNF complex subunit (m-BAF155; 1:1,000; 94962; Cell Signaling, Danvers, MA, USA), AMDA-marked polyadenylate-binding protein 1 (m-PABP1; 1:1,000; 3505S; Cell Signaling), PABP1 (1:1,000; 4992S; Cell Signaling), peroxisome proliferator-activated receptor gamma coactivator-1a (PGC-1a; 1:1,000; AB3242; EMD Millipore, Darmstadt, HE, Germany), complexes I-V of mitochondrial oxidative phosphorylation (OXPHOS; 1:1,000; ab110413; Abcam, Cambridge, UK), muscle RING-finger protein-1 (MuRF1; 1:200; AF5366; 140 R&D Systems, Minneapolis, MN, USA), muscle atrophy F-box (MAFbx; 1:1,000; AP2041; ECM Biosciences, Versailles, KY, USA), ubiquitin-binding protein 62 (p62; 1:1,000; P0067; Sigma Aldrich), BCL2 interacting protein 3 (Bnip3; 1:1,000; 3769S; Cell Signaling), microtubule-associated protein 1A/1B-light chain 3 (LC3;1:1,000; 4108S; Cell

Signaling), phosphorylated 4E-binding protein-1 (p-4EBP1$^{Thr37/46}$; 1:1000; 2855S; Cell Signaling), 4EBP1 (1:1,000; 9452S; Cell Signalling), p- ribosomal protein s6 (s6$^{Ser235/236}$; 1:1,000; 2211S; Cell Signaling), and s6 (1:1,000; 2217S; Cell Signaling).

RNA isolation and real-time polymerase chain reaction (RT-qPCR). RNA was isolated from frozen, powdered GAST muscle. All samples were homogenized in 1 mL of Trizol reagent (Invitrogen; Carlsbad, CA, USA) using stainless steel lysing beads and placed in the Tissue Lyser (Qiagen) to run for 5 bouts of 30 seconds at a frequency of 20.0 1/second. Homogenized samples were then mixed with 200 mL of chloroform (Thermo Fisher Scientific; Waltham, MA, USA), agitated vigorously for 15 seconds and centrifuged at 12,000 g for 10 minutes. The upper aqueous (RNA) phase was purified using the E.Z.N.A Total RNA kit (VWR International; Radnor, PA, USA) as per the instructions provided by the manufacturer. RNA concentration and purity were determined using the NanoDrop 1000 Spectrophotometer (Thermo Fisher Scientific). RNA samples were then reverse transcribed into cDNA using a high-capacity cDNA reverse transcription kit (Thermo Fisher Scientific) according to the manufacturer instructions. All individual RT-qPCRs were run in triplicate 6 mL reactions containing GoTaq qPCR Master Mix (Promega; Madison, WI, USA). Data were analyzed using the comparative CT method (Schmittgen & Livak, 2008). TBP and GAPDH were used as control housekeeping genes for all experiments, as the average of their CT values did not change between experimental conditions (data not shown). The following primers (Sigma Aldrich) were used in this study: CARM1 F-CAACAGCGTCCTCATCCAGT, R-

GTCCGCTCACTGAACACAGA, fibroblast growth factor-binding protein (FGFBP1) F-ACACTCACAGAAAGGTGTCCA, R-CTGAGAACGCCTGAGTAGCC.

Immunofluorescence microscopy. SOL muscles stored in OCT were sectioned into 10 mm slices on a cryostat (Thermo Fisher Scientific) at -20 °C. Prior to staining, samples were air dried for ~30 minutes and subsequently incubated in 10% goat serum in PBS to prevent non-specific binding. Staining of myosin heavy chain isoforms (MHC) was performed as previously described (Bloemberg & Quadrilatero, 2012) using primary antibodies against MHC I (BA-F8), MHC IIa (SC-71), and MHC IIb (BF-F3) (Developmental Studies Hybridoma Bank, Iowa City, IA, USA), followed by isotype-specific fluorescent secondary antibodies (Invitrogen, Carlsbad, CA, USA). This allowed for the identification of type I, type IIa, type IIb, type IIx and hybrid muscle fibres. All slides were viewed with the Nikon Eclipse Ti Microscope (Nikon Instruments, Mississauga, ON, Canada), equipped with a high resolution Photometrics CoolSNAP HQ2 fluorescent camera. Images were captured and analyzed using the Nikon NIS Elements AR 3.2 software. All images were obtained with the 20x objective. For each sample, all fibres of every type were counted to obtain fibre type percentage. The fibres within a pre-determined region of interest (which excluded exterior and elongated fibres) were manually circled to determine fibre-type specific cross-sectional area (CSA). Investigators performing counting and circling were blinded to the experimental conditions.

Statistical Analyses. All statistical analyses were completed on Prism. A two-way analysis of variance (ANOVA) was performed to examine main effects of treatment (EZM vs. Veh) and sex (male vs. female), as well as any interactions between variables, for

protein content, muscle mass, and functional measures in Figures 1 and 2. In Figures 3, 7, and 8, when there was no difference in percentage change in protein or mRNA content between male and female mice in response to DEN, male and female data were pooled to increase our statistical power to detect true effects of experimental conditions. Subsequently, a two-way ANOVA was completed to investigate the main effects of treatment and DEN, and interactions between variables. A three-way ANOVA was performed to examine the main effects of treatment, sex, and DEN (CON vs. DEN) and interactions between variables, for body and muscle mass in Figure 4. In Figures 5 and 6, a two-way ANOVA was completed separately in male and female mice to assess main effects of DEN and treatment, as well as interactions between variables. Šidák multiple comparisons tests were performed when main effects and/or interactions were identified. Statistical differences were considered significant if $p < 0.05$. Data are presented as mean +/- SEM.

Results

Pharmacological CARM1 inhibition reduces CARM1 methyltransferase activity in skeletal muscle. To examine the effects of global, pharmacological CARM1 inhibition on skeletal muscle biology, adult male and female mice (n = 10-11/sex) were treated with either EZM (150 mg/kg) or Veh compound for 11-13 days (Figure 1A). On the 10^{th} day of treatment, a variety of functional tests were completed on all mice. The animals treated for 11 days were euthanized on day 11, while the cohort of remaining mice performed a single bout of treadmill running on day 11 to assess exercise capacity and their tissues were

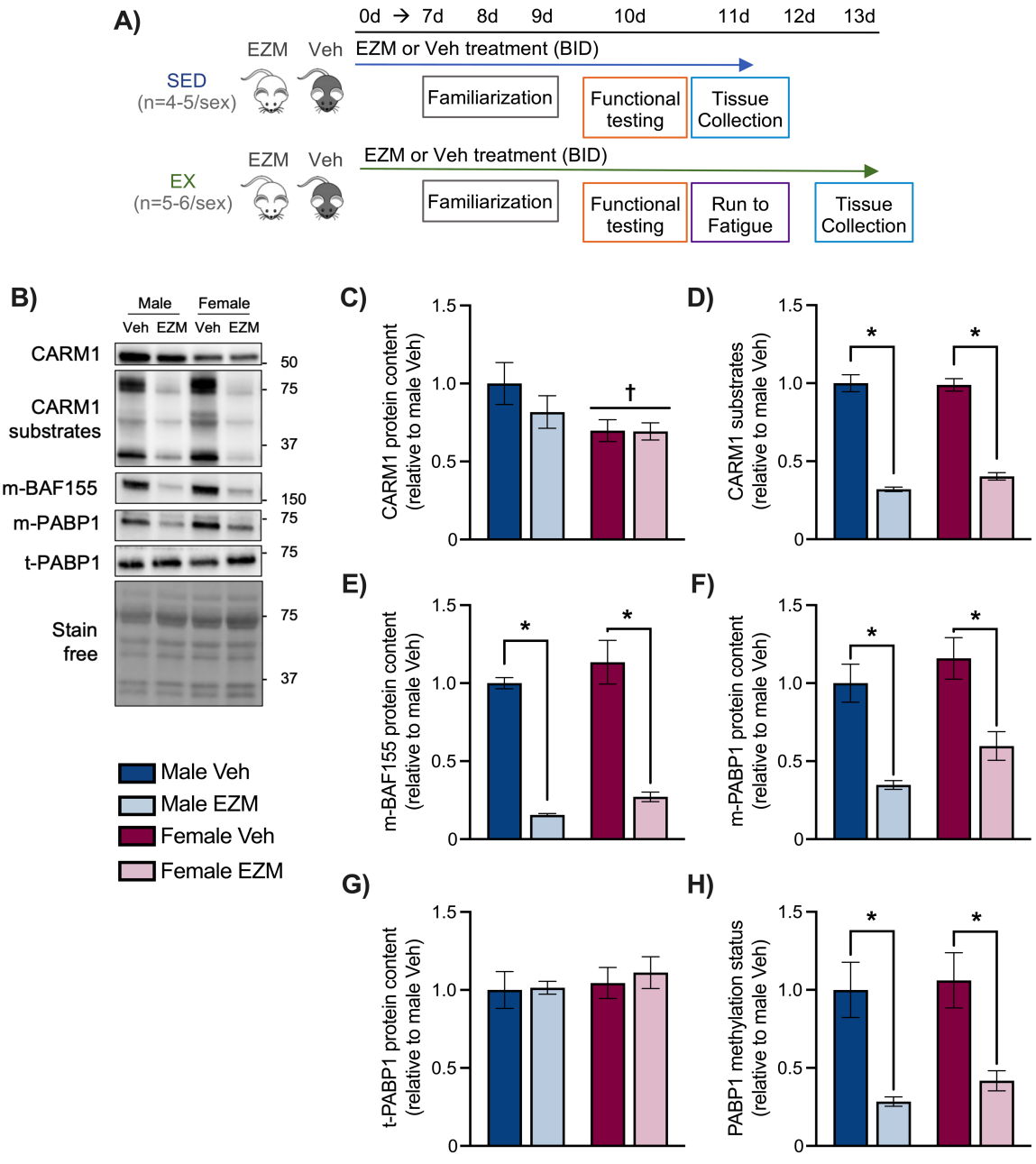

Figure 1: EZM inhibits CARM1 in skeletal muscle. (A) Experimental design for the first arm of this study. (B) Typical Western blots of CARM1, CARM1 substrates, m-BAF155, m-PABP1, and t-PABP1 protein in GAST muscles of male and female mice after 11-13 days of daily Veh or EZM (150 mg/kg) treatment. A stain free image of the membrane is shown to demonstrate equal sample loading. Approximate molecular weights (kDa) are displayed at right of blots. Graphical summaries of (C) CARM1 protein, (D) CARM1 substrates, (E) m-BAF155, (F) m-PABP1, (G) t-PABP1, and (H) PABP1 methylation status (i.e., the methylated form of the protein relative to its total amount), expressed relative to the male Veh-treated group. Bar graphs are expressed as mean +/- SEM. Two-way ANOVA; *, $p < 0.05$ versus Veh; †, main effect of sex. n = 10-11.

collected on day 13. Our pilot experiments demonstrated that 4 days of EZM administration was effective at significantly decreasing asymmetric dimethylation of arginine residues on CARM1 substrates by 85% in liver and 70% in skeletal muscle (data not shown). We sought to investigate CARM1 biology in muscle following a longer duration of EZM exposure. We performed immunoblot analyses of CARM1, and its known targets, including PABP1, BAF155, and CARM1 substrates in the GAST muscles of Veh- and EZM-treated male and female animals. We observed a main effect of sex, where skeletal muscle CARM1 content was 25% lower in female versus male mice (Figure 1B, C). CARM1 content was unaffected by EZM administration. ADMA-marked CARM1 substrates and methylated BAF155 levels were decreased ($p < 0.05$) by 65-80% in EZM-treated male and female mice compared to Veh-treated animals (Figure 1B, D, E). EZM significantly reduced asymmetrically dimethylated PABP1 content and PABP1 methylation status (i.e., the methylated form of the protein expressed relative to the total protein content) by 50-75% in both sexes versus Veh-dosed mice (Figure 1B, F-H).

Pharmacological inhibition of CARM1 does not affect body or skeletal muscle mass but impairs muscle function in a sex-specific manner. Next, we analyzed body mass in response to EZM administration and found that it was unchanged after 11 days of treatment (Figure 2A). EZM-treated male mice had significantly reduced GAST muscle mass, as compared to Veh-treated males, whereas female mice treated with EZM demonstrated a greater ($p < 0.05$) GAST mass versus their sex-matched Veh counterparts (Figure 2B). However, the mass of several other lower limb muscles was not affected by EZM. Grip strength and grip fatigue were similar between EZM- and Veh-treated mice (Figure 2C-E).

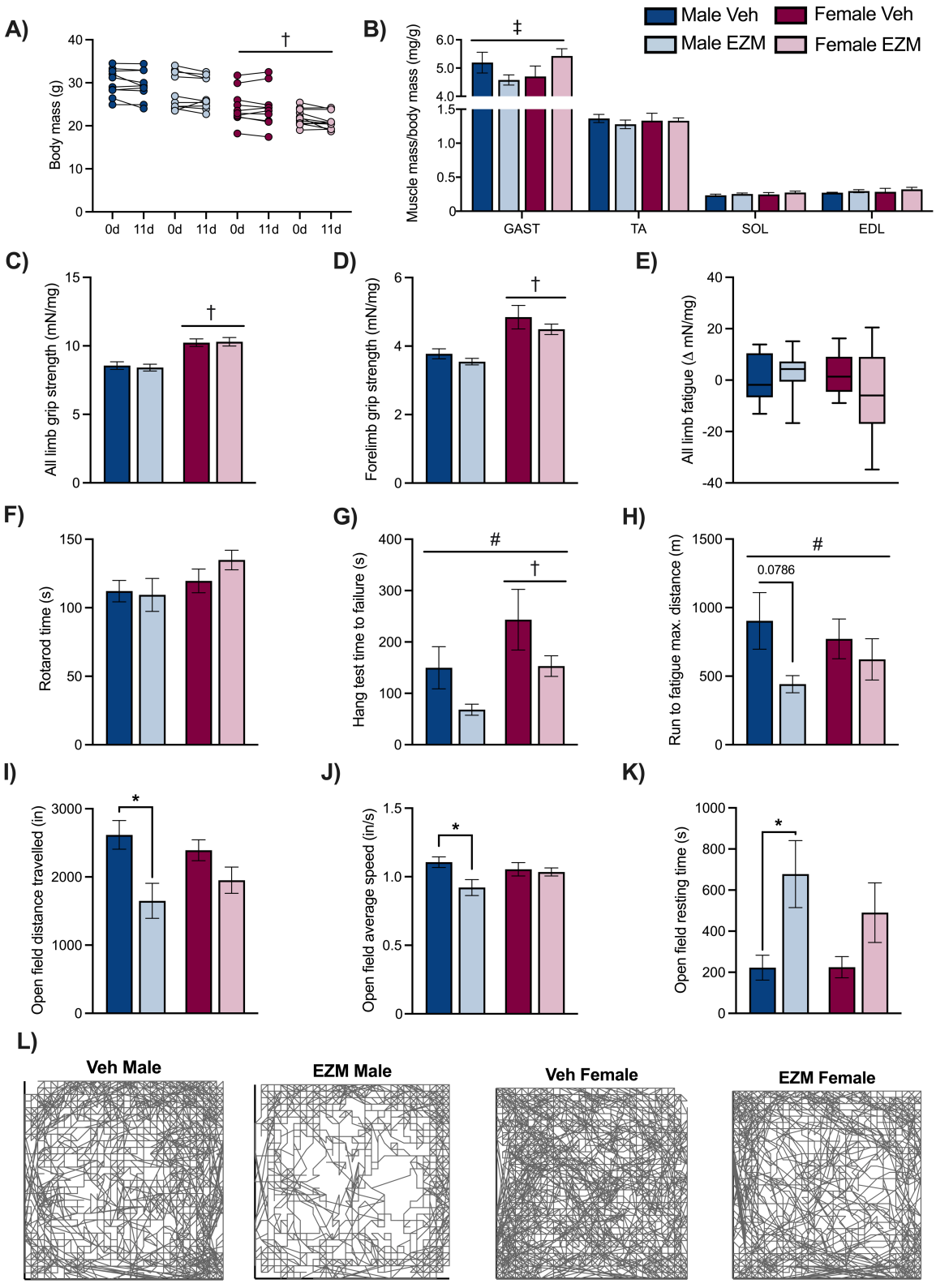
A)
Body mass (g)
0d
11d
†
B)
Male Veh
Female Veh
Male EZM
Female EZM
Muscle mass/body mass (mg/g)
‡
GAST
TA
SOL
EDL
C)
All limb grip strength (mN/mg)
D)
Forelimb grip strength (mN/mg)
E)
All limb fatigue (Δ mN/mg)
F)
Rotarod time (s)
G)
Hang test time to failure (s)
#
H)
Run to fatigue max. distance (m)
0.0786
I)
Open field distance travelled (in)
*
J)
Open field average speed (in/s)
K)
Open field resting time (s)
L)
Veh Male
EZM Male
Veh Female
EZM Female

Figure 2: Daily CARM1 inhibition impacts skeletal muscle function, exercise capacity, and movement behaviours. (A) Body mass of male and female mice at zero and eleven days of treatment with EZM or Veh compound. (B) Mass of gastrocnemius (GAST), tibialis anterior (TA), soleus (SOL), and extensor digitorum longus (EDL) muscles expressed relative to body mass (mg/g) of male and female EZM and Veh-treated mice. Maximum (C) all limb and (D) forelimb grip strength expressed relative to body weight (mN/mg). (E) All-limb grip fatigue (Δ mN/mg). (F) Maximum run time (s) during rotarod test. (G) Time to failure (seconds; s) during hang test. (H) Maximum distance travelled (metres; m) during treadmill exercise. (I-K) Distance travelled (inches; in), average speed (inches/second; in/s), and resting time (s) in the four experimental groups during a 60-minute open field tracking period. (L) Representative tracings of movement patterns during open field test. Bars are mean +/- SEM. Boxes represent 25th and 75th percentiles, line is mean, and bars represent maximum and minimum. †, main effect of sex; ‡, sex and treatment interaction #, main effect of treatment; p-values displayed for Veh vs. EZM. N = 10-11 in panels A-K. n = 5-6 in panel H.

Muscular endurance and coordination were assessed via the hang and rotarod tests (Aartsma-Rus & van Putten, 2014; Manta et al., 2019). Rotarod performance was similar across treatment groups and sex (Figure 2F). In contrast, we observed significant main effects of treatment and sex in the time to failure during the hang test, where EZM-treated female and male mice fatigued 40-55% earlier than Veh-treated animals (Figure 2G). Male EZM-treated mice tended to run less ($p = 0.08$) than Veh-treated male mice during the treadmill test, whereas exercise capacity was similar between female Veh and EZM groups (Figure 2H). We next examined the effects of pharmacological CARM1 inhibition on locomotor and exploratory behaviours by monitoring the activity of mice during a one-hour tracking period in an open-field chamber (Gould et al., 2009). EZM-dosed male mice demonstrated significantly lower movement speed, less distance traveled, and more sedentary time compared to their sex-matched Veh-treated littermates (Figure 2I-L). In contrast, there was no difference in open-field parameters between treatment groups in female mice.

Pharmacological CARM1 inhibition attenuates increased CARM1 methyltransferase activity following denervation. We sought to explore the impact of

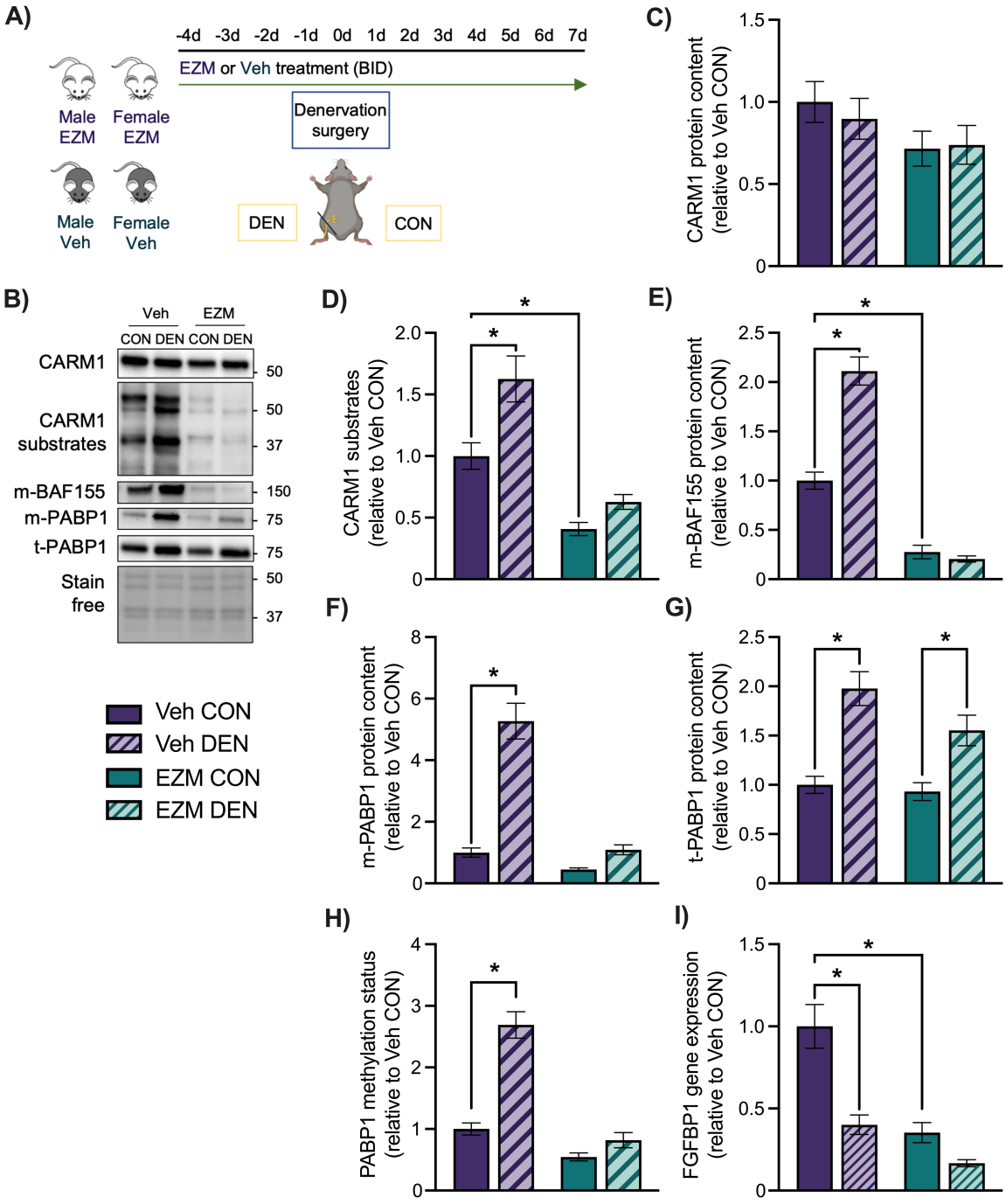
A)
-4d -3d -2d -1d 0d 1d 2d 3d 4d 5d 6d 7d
EZM or Veh treatment (BID)
Denervation surgery
Male EZM
Female EZM
Male Veh
Female Veh
DEN
CON
B)
Veh
EZM
CON DEN CON DEN
CARM1
CARM1 substrates
m-BAF155
m-PABP1
t-PABP1
Stain free
50
50
37
150
75
75
50
37
Veh CON
Veh DEN
EZM CON
EZM DEN
C)
CARM1 protein content (relative to Veh CON)
D)
CARM1 substrates (relative to Veh CON)
E)
m-BAF155 protein content (relative to Veh CON)
F)
m-PABP1 protein content (relative to Veh CON)
G)
t-PABP1 protein content (relative to Veh CON)
H)
PABP1 methylation status (relative to Veh CON)
I)
FGFBP1 gene expression (relative to Veh CON)

Figure 3: Pharmacological CARM1 inhibition attenuates increases in CARM1 methyltransferase activity following 7 days of denervation-induced neurogenic disuse. (A) Experimental design for the second arm of this study. (B) Representative Western blots of CARM1, CARM1 substrates, m-BAF155**,** m-PABP1, and t-PABP1 in GAST muscles of the non-denervated, control (CON) and contralateral denervated (DEN) limbs of Veh- and EZM-treated mice. A stain-free image of the membrane is shown to demonstrate consistent loading. Approximate molecular weights (kDa) are displayed at right of blots. Graphical summaries of (C) CARM1, (D) CARM1 substrates, (E) m-BAF155, (F) m-PABP1, (G) t-PABP1, and (H) PABP1 methylation status expressed relative to Veh CON. Graphical summaries of mRNA expression in GAST muscles of (I) FGFBP1 shown relative to Veh CON. Male and female data were pooled because there was no significant difference between sexes in the percentage change in these outcome measures in response to DEN (data not shown). Bar graphs are expressed as mean +/- SEM. Two-way ANOVA; *, $p < 0.05$ between indicated groups. n = 15-16.

pharmacological CARM1 inhibition on denervation-induced muscle atrophy. Female and male mice were pre-treated for 4 days with either EZM or Veh compounds, and on day 5 of treatment, unilateral sectioning of the sciatic nerve was performed (Stouth et al., 2018, 2020) to rapidly evoke neurogenic muscle atrophy in one limb, while maintaining a contralateral, innervated intra-animal control limb (Figure 3A). The Veh/EZM course continued for another 7 days, and animals were euthanized on day 11. To investigate whether CARM1 inhibition was effective at mitigating elevations in CARM1 methyltransferase activity following DEN, we immunoblotted CARM1 and its substrates in control (CON) and denervated (DEN) GAST muscles of Veh- and EZM-treated male and female mice. To increase our statistical power to detect effects of EZM treatment and DEN, male and female data were pooled because there were no significant differences between sexes in the percentage change of these outcome metrics in response to DEN (data not shown). CARM1 protein content was unaffected by DEN in either treatment group, although it tended to be reduced ($p = 0.07$) in EZM-dosed mice (Figure 3B, C). ADMA-marked CARM1 substrates and BAF155 were significantly elevated 1.6- and 2-fold

respectively in the DEN muscles of Veh-treated, but not in EZM-treated mice (Figure 3B, D, E). Similarly, ADMA-marked PABP1 was increased ($p < 0.05$) 5-fold in DEN GAST muscle compared to CON in Veh-dosed mice, however, this induction was significantly attenuated in EZM-dosed mice (Figure 3B, F). Total PABP1 levels were 1.6-2-fold greater ($p < 0.05$) in DEN versus CON muscles of both groups, with no difference between Veh and EZM administration (Figure 3B, G). EZM significantly blunted the elevation in PABP1 methylation status observed in DEN muscles of Veh-treated mice (Figure 3H). vanLieshout and colleagues recently identified several genes that were differentially expressed in the skeletal muscles of CARM1 mKO mice compared to their wildtype (WT) littermates, indicating that these transcripts were regulated by CARM1 (vanLieshout et al., 2022). Specifically, mRNA levels of FGFBP1 were reduced by ~95% ($p < 0.05$) in CARM1 mKO mice. Similarly, here we found that FGFBP1 mRNA expression was significantly 65% lower in the CON muscle of EZM-treated mice compared to their Veh-treated counterparts and was decreased ($p < 0.05$) following DEN in both treatment groups (Figure 3I).

Denervation-induced muscle mass loss is unaffected by pharmacological CARM1 inhibition. We investigated the effect of global, pharmacological CARM1 inhibition on body and skeletal muscle mass in response to DEN-induced muscle atrophy. We found that EZM-dosed male mice had significantly lower body mass post-DEN versus pre-DEN, while the other treatment groups exhibited no change in body mass in response to neurogenic disuse (Figure 4A). There was a 15-20% reduction ($p < 0.05$) in DEN GAST muscle mass, expressed relative to body mass, compared to its innervated, contralateral CON across all groups except the male Veh cohort, which demonstrated a strong statistical

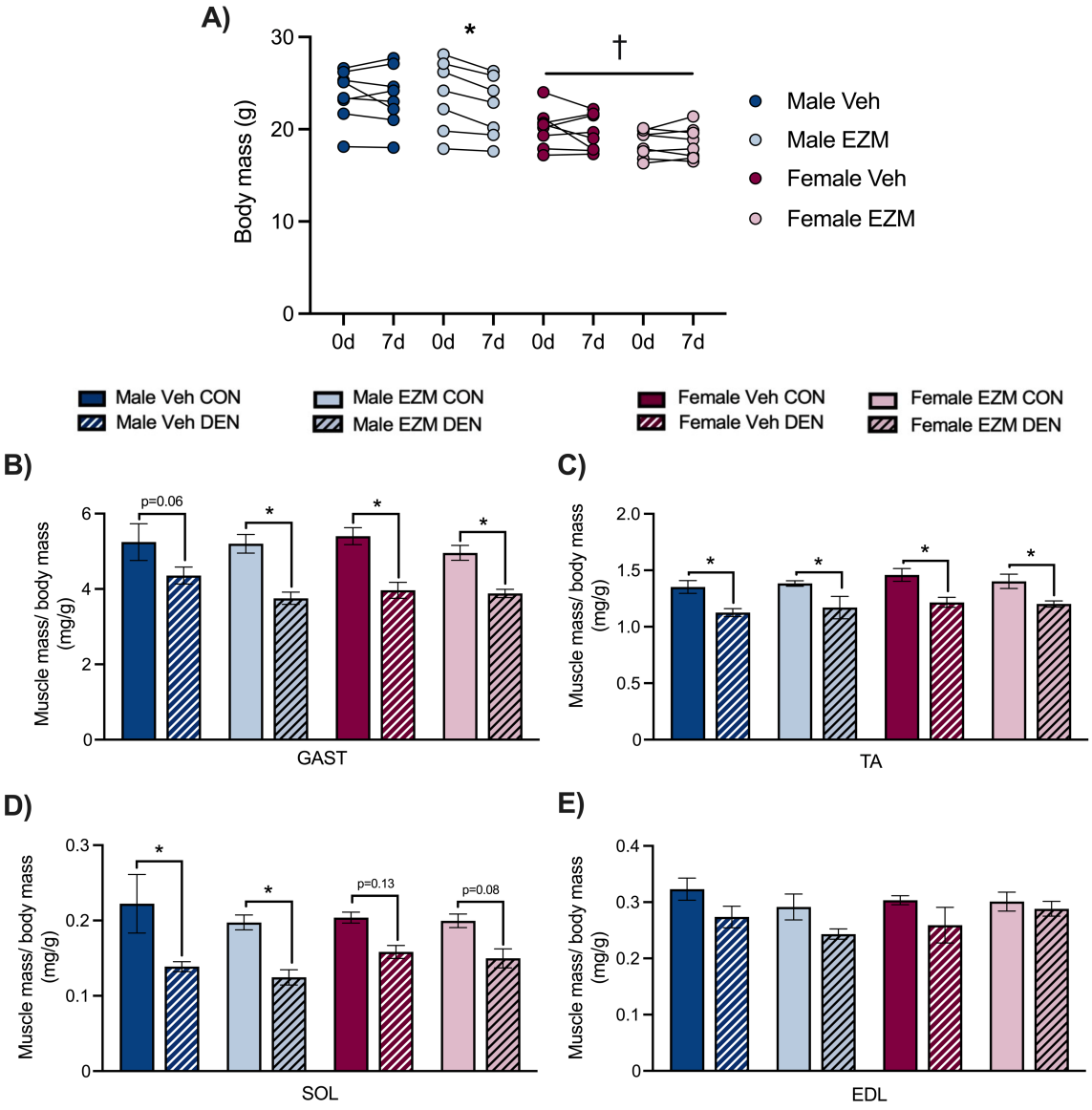

Figure 4: CARM1 inhibition does not influence denervation-induced muscle mass loss. (A) Graphical summary of body mass (g) before DEN surgery (0d) and after surgery (7d) in male and female mice receiving EZM or Veh. Summaries of muscle mass expressed relative to body mass (mg/g) in (B) GAST, (C) TA, (D) SOL, and (E) EDL in the CON and DEN limbs of mice across the four experimental groups. Male and female data were pooled because there was no significant difference between sexes in the percentage change in these outcome measures in response to DEN (data not shown). Bar graphs are mean +/- SEM. Three-way ANOVA; *, $p < 0.05$ between indicated groups; P-values shown when approaching $p < 0.05$; †, main effect of sex. n = 7-8.

trend ($p = 0.06$; Figure 4B). TA muscle mass was significantly reduced by ~15% in the DEN versus CON limbs in Veh- and EZM-treated mice of both sexes (Figure 4C). DEN significantly decreased SOL muscle mass in all male mice, however a statistical trend ($p < 0.13$) for SOL mass reduction in DEN compared to CON legs was observed in female animals (Figure 4D). EDL muscle mass was not affected by neurogenic disuse (Figure 4E).

Denervation reduces muscle fibre size independent of pharmacological CARM1 inhibition. Next, we examined the influence of DEN on muscle fibre-specific CSA and fibre type composition distribution to determine whether these factors were affected by CARM1 inhibition. Following 7 days of DEN, SOL muscle fibres appear smaller and more angular than CON fibres (Figure 5A). In female mice, all fibre types exhibited a significant decrease in CSA after DEN that was independent of CARM1 inhibition (Figure 5A-D). Similarly, the CSA of myosin heavy chain (MHC) type I, IIa, and IIx DEN fibres in male mice was also reduced ($p < 0.05$) relative to CON fibres in both EZM- and Veh-treated groups (Figure 5A, E-G). The SOL muscles of female mice had the following distribution of MHC I, IIa, IIx, IIb and hybrid fibres: 48%, 40%, 7%, 1%, 4%, whereas the SOL muscle of male mice had the following distribution: 37%, 50%, 8%, 1%, 4% (Figure 6A, B). There was no significant effect of DEN or EZM treatment on fibre type distribution in either sex. In male and female mice, there was an interaction between DEN and size of MHC I, IIa, and IIx fibres, such that a greater percentage of fibres in DEN muscle had smaller CSA than in CON muscle (Figure 6C-H). In type I fibres of female mice, EZM CON muscles

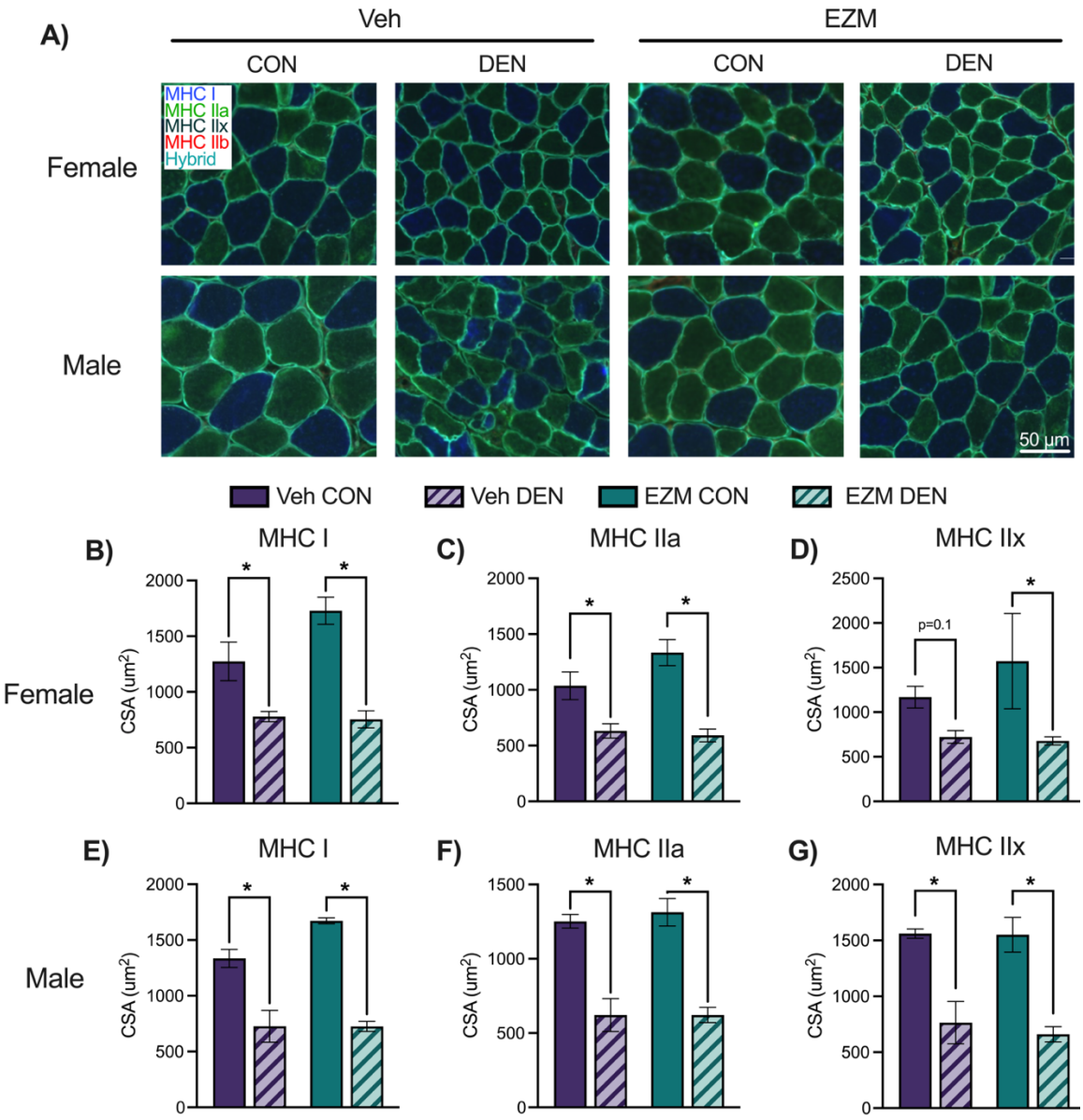

Figure 5: Denervation decreases muscle fibre cross-sectional area independent of pharmacological CARM1 inhibition. (A) Representative images of immunofluorescence fibre-type staining of soleus muscles, including laminin (cyan), myosin heavy chain (MHC) type I (blue), MHC type IIa (green), and MHC IIx (red). Type IIx fibres were unstained and hybrid fibres appear as a blue/green hybrid. Graphical summary of average cross-sectional area (CSA; um^2) of (B) MHC I, (C) MHC IIa, and (D) MHC IIx fibres of DEN and CON muscle sections from female EZM and Veh-treated mice. Graphical summary of average CSA of (E) MHC I, (F) MHC IIa, and (G) MHC IIx-stained fibres of DEN and CON muscle sections from male EZM and Veh-treated mice. Data are expressed as mean +/- SEM. Two-way ANOVA; *, $p < 0.05$ between indicated groups; P-values shown when approaching $p < 0.05$. $n = 4$.

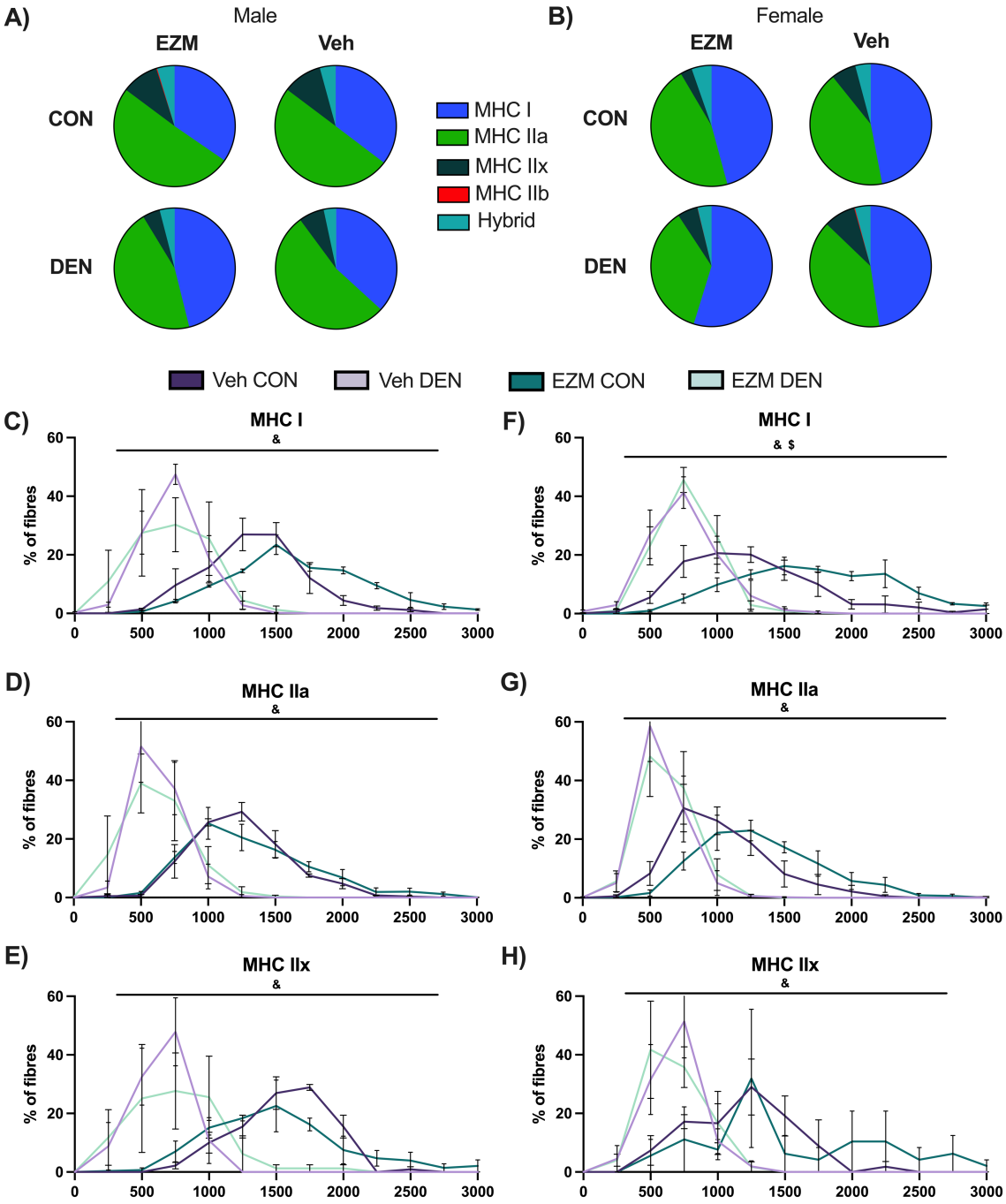
A)
Male
EZM
Veh
CON
DEN
MHC I
MHC IIa
MHC IIx
MHC IIb
Hybrid
B)
Female
EZM
Veh
CON
DEN
Veh CON
Veh DEN
EZM CON
EZM DEN
C)
MHC I
&
F)
MHC I
& $
D)
MHC IIa
&
G)
MHC IIa
&
E)
MHC IIx
&
H)
MHC IIx
&
% of fibres
0
20
40
60
0
500
1000
1500
2000
2500
3000

Figure 6: CARM1 inhibition does not influence fibre type composition distribution. Pie charts of fibre type distribution CON and DEN SOL muscles of (A) male, and (B) female EZM and Veh-treated mice. (C-E) Fibre size distribution of type I, type IIa, and type IIx fibres in CON and DEN muscles of male mice. (F-H) Fibre size distribution of type I, type IIa, and type IIx fibres in CON and DEN muscles of female mice. Data are expressed as mean +/- SEM. Two-way ANOVA for panels A&B; Three-way ANOVA for panels C-H; &, size and DEN interaction, $, size and drug interaction. n = 4

tended to have more large fibres compared to Veh CON, an effect that was not apparent in the DEN muscles (Figure 6F).

Pharmacological CARM1 inhibition affects mitochondrial protein profile in response to denervation. We then studied, during neurogenic atrophy, the effect of CARM1 inhibition on skeletal muscle PGC-1α, a regulator of mitochondrial biogenesis. PGC-1α content was lower ($p < 0.05$) in DEN muscles of both EZM and Veh-treated mice relative to the CON condition (Figure 7A, B). We also examined the expression of OXPHOS complexes I-V (CI-CV). We observed a significant ~20% reduction in CI content in DEN muscles compared to CON in both Veh- and EZM-treated groups, however, CIII and CIV levels were only decreased ($p < 0.05$) in DEN muscles of EZM-dosed mice, while CII and CV were similar between all groups (Figure 7C). When the data for CI-CV were pooled, DEN lowered OXPHOS expression by 10-15% in Veh- and EZM-treated mice, but the reduction was statistically significant only in the EZM groups (Figure 7C).

Molecular regulators of skeletal muscle mass are elevated following denervation independently of pharmacological CARM1 inhibition. Finally, we investigated the effects of pharmacological CARM1 inhibition on several molecules that are well-characterized mediators of skeletal muscle mass. Muscle-specific ubiquitin ligases, MuRF1 and MAFbx, were significantly upregulated 2-4-fold respectively in DEN relative to CON muscles in

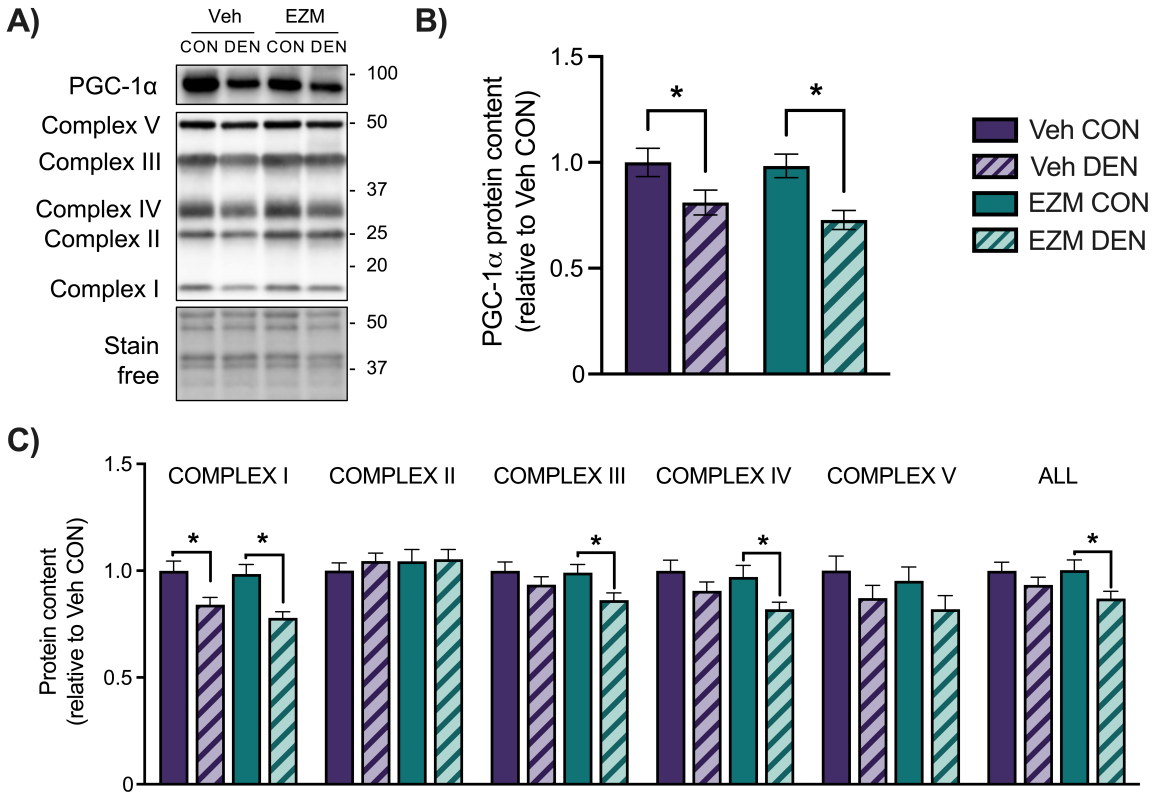

Figure 7: CARM1 inhibition affects the mitochondrial protein profile in response to denervation. (A) Typical Western blots of peroxisome proliferator-activated receptor gamma coactivator-1a (PGC-1α) and representative subunits of mitochondrial oxidative phosphorylation (OXPHOS) protein complexes (Complex I-V) in GAST muscles from CON and DEN muscles of Veh and EZM-treated mice. A stain-free image of the membrane is shown to demonstrate consistent loading. Approximate molecular weights (kDa) are displayed at right of blots. Graphical summaries of (B) PGC-1a, and (C) mitochondrial Complex I-V protein levels in CON and DEN limbs of EZM and Veh-treated mice. Data are expressed relative to vehicle control condition. Male and female data were pooled because there was no significant difference between sexes in the percentage change in these outcome measures in response to DEN (data not shown). Bar graphs are mean +/- SEM. Two-way ANOVA; *, $p < 0.05$ between indicated groups. n = 15-16.

both treatment groups, with no difference between Veh and EZM (Figure 8A-C). Proteins that are indicative of autophagy and mitophagy, p62 and BNIP3, were also elevated ~2-fold ($p < 0.05$) in DEN muscles and were unaffected by pharmacological CARM1 inhibition (Figure 8A, D, E). We also examined LC3, an autophagosome membrane protein that is converted from LC3 I to LC3 II during the formation of autophagosomes

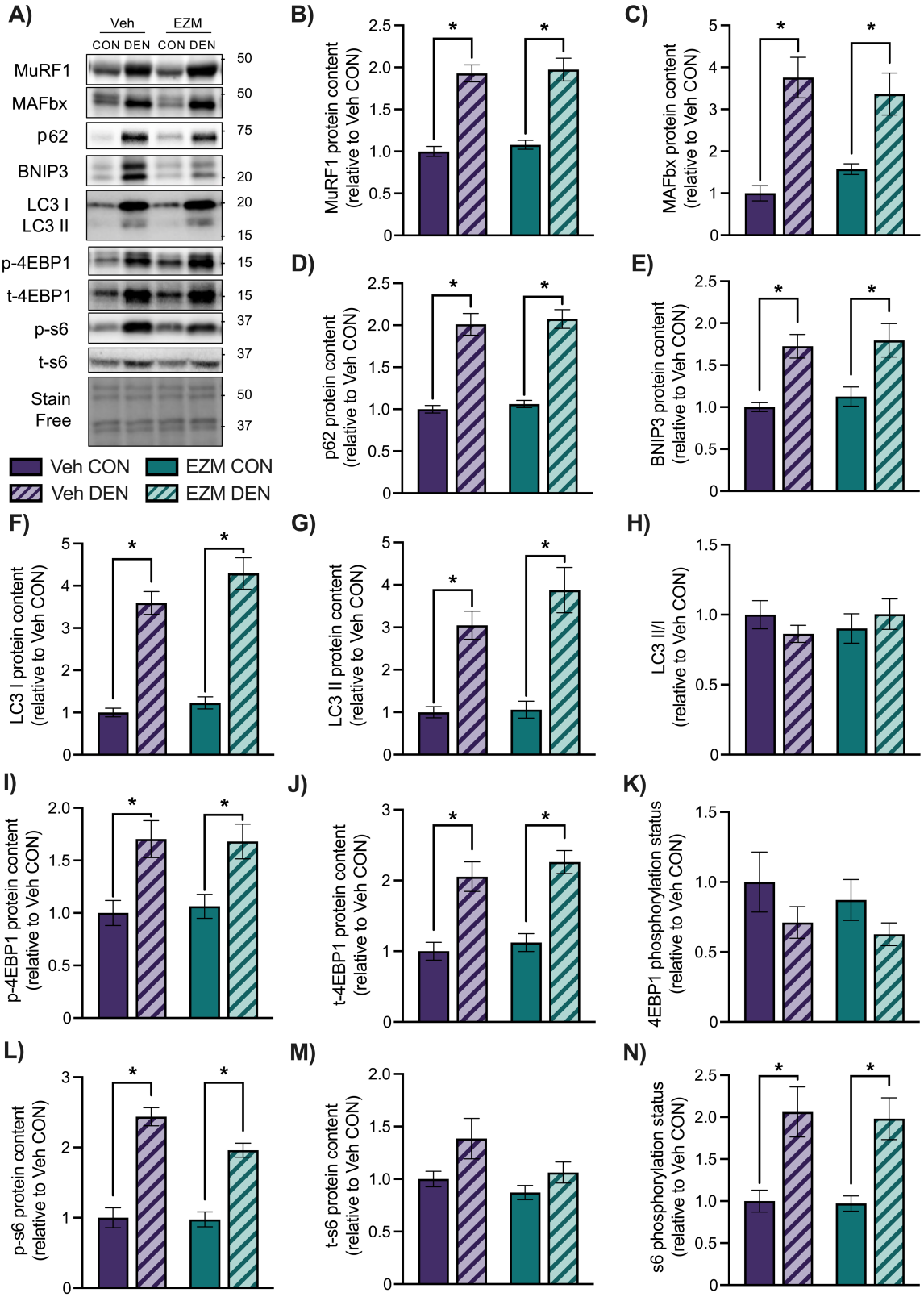
A)
Veh
EZM
CON DEN CON DEN
MuRF1
MAFbx
p62
BNIP3
LC3 I
LC3 II
p-4EBP1
t-4EBP1
p-s6
t-s6
Stain Free
50
50
75
20
20
15
15
15
37
37
50
37
Veh CON
EZM CON
Veh DEN
EZM DEN
B)
MuRF1 protein content (relative to Veh CON)
C)
MAFbx protein content (relative to Veh CON)
D)
p62 protein content (relative to Veh CON)
E)
BNIP3 protein content (relative to Veh CON)
F)
LC3 I protein content (relative to Veh CON)
G)
LC3 II protein content (relative to Veh CON)
H)
LC3 II/I (relative to Veh CON)
I)
p-4EBP1 protein content (relative to Veh CON)
J)
t-4EBP1 protein content (relative to Veh CON)
K)
4EBP1 phosphorylation status (relative to Veh CON)
L)
p-s6 protein content (relative to Veh CON)
M)
t-s6 protein content (relative to Veh CON)
N)
s6 phosphorylation status (relative to Veh CON)

Figure 8: Molecular regulators of skeletal muscle size are elevated following denervation independent of pharmacological CARM1 inhibition. (A) Representative Western blots of muscle RING-finger protein-1 (MURF1), muscle atrophy F-box (MAFbx), ubiquitin-binding protein 62 (p62), BCL2 interacting protein 3 (BNIP3), microtubule-associated protein 1A/1B-light chain 3 (LC3 I and II), phosphorylated 4E-binding protein-1 (p-4EBP1), total 4EBP1 (t-4EBP1), phosphorylated ribosomal protein s6 (p-s6), and total s6 (t-s6) in CON and DEN limbs of Veh- and EZM-treated mice. A representative stain free image of the membrane is shown below to demonstrate equal sample loading. Approximate molecular weights (kDa) are displayed at right of blots. Graphical summaries of (B) MURF1, (C) MAFbx, (D) p62, (E) BNIP3, (F) LC3 I, (G) LC3 II, (H) LC3 II/I ratio, (I) p-4EBP1, (J) t-4EBP1, (K) 4EBP1 phosphorylation status, (L) p-s6, (M) t-s6, and (N) s6 phosphorylation status in CON and DEN limbs of both treatment groups expressed relative to the Veh CON cohort. Male and female data were pooled because there was no significant difference between sexes in the percentage change in these outcome measures in response to DEN (data not shown). Data are expressed as mean +/- SEM. Two-way ANOVA; *, $p < 0.05$ between indicated groups. n = 12-16.

(Tanida et al., 2008), in response to DEN and EZM. We found that LC3 I and II were robustly increased ($p < 0.05$) in DEN muscles compared to CON to a similar extent between Veh and EZM groups, however, the LC3II-to-LC3-I ratio was unaffected (Figure 8A, F-H). Finally, we measured downstream targets of mammalian target of rapamycin (mTOR), s6 and 4EBP1, as molecular outputs of mTOR activity during neurogenic muscle atrophy. Phosphorylated and total 4EBP1 levels were significantly greater in DEN versus CON muscles with no difference between Veh and EZM administration, whereas 4EBP1 phosphorylation status was similar across all groups (Figure 8A, I-K). Phosphorylated and total s6 were increased more in DEN muscles of Veh-treated mice than EZM-treated mice, however s6 phosphorylation status was similar between treatment groups (Figure 8A, L-N).

Discussion

The purpose of the present study was to further investigate the role of CARM1 in the maintenance and plasticity of skeletal muscle mass and function at rest and during neurogenic muscle atrophy. Our data demonstrate that short-term treatment with an orally bioavailable, CARM1 inhibiting compound was effective at reducing CARM1 activity in skeletal muscle. The decrease in CARM1 methyltransferase function corresponded with impaired muscular endurance and exercise capacity, particularly in male mice, despite only minimal changes to body mass and muscle mass. DEN augmented the methylation of CARM1 substrates in skeletal muscle of Veh-treated mice, but this response was abolished in EZM-treated animals. Nevertheless, DEN-induced decreases in skeletal muscle mass and myofibre CSA occurred to a similar degree in males and females irrespective of CARM1 activity. Accordingly, the molecular muscle atrophy and autophagy programs were upregulated following DEN independent of CARM1 methylating capacity. Collectively, these data demonstrate that pharmacological CARM1 inhibition markedly reduced CARM1 activity in skeletal muscle while eliciting alterations in muscle and whole-body physical function in the absence of changes in muscle mass and myofibre CSA. Furthermore, short-term CARM1 suppression had no impact on DEN-evoked muscle atrophy. These findings, along with other recent work (Liu et al., 2019; Stouth et al., 2018, 2020; vanLieshout et al., 2022), together indicate specific spatiotemporal effects of CARM1 content and activity in the maintenance and remodelling of skeletal muscle biology.

We employed a novel pharmacological strategy that targets CARM1 to further evaluate the role of the methyltransferase in skeletal muscle of adult animals. While not without drawbacks such as broad, "off-target" tissue pharmacokinetics, this methodology circumvents the major limitations associated with common genetic approaches utilizing full-body or skeletal muscle-specific CARM1 KO (Kim et al., 2010; Stouth et al., 2020; vanLieshout et al., 2022; Yadav et al., 2003). Furthermore, the CARM1 inhibitor EZM is orally bioactive, highly specific, and safe in several pre-clinical contexts (Drew et al., 2017; Greenblatt et al., 2018; Kumar et al., 2021; Veazey et al., 2020; Zhang et al., 2021), and therefore represents an effective and practical tool compound with significant translational potential (Q. Wu et al., 2021). EZM directly binds to CARM1 at the peptide-substrate binding site to prevent methylation but does not contribute to the degradation of the enzyme (Zhang et al., 2021). As such, muscle CARM1 protein content was not different between Veh- and EZM-treated animals. On the other hand, EZM administration significantly decreased markers of skeletal muscle CARM1 activity, including specific BAF155 and PABP1 methylation and general asymmetric dimethylation of CARM1 substrates, by 55-80% compared to Veh-treated animals. In fact, this EZM-evoked reduction in GAST muscle CARM1 arginine methyltransferase activity was greater than that observed in the TA muscle of CARM1 mKO mice as compared to age- and sex-matched wild-type littermates [-40-65% (Stouth et al., 2020; vanLieshout et al., 2022)], which is likely due to the added inhibition by EZM of CARM1 in muscle-resident non-myogenic cells. We also show that global CARM1 inhibition under basal conditions did not influence body mass in female or male animals, in agreement with previous studies of healthy and diseased mice

after varying lengths of treatment (Drew et al., 2017; Greenblatt et al., 2018; Veazey et al., 2020; Zhang et al., 2021). However, while muscle strength was unaffected by CARM1 inhibition, in contrast, motor performance, movement behaviours, and exercise capacity were impacted, particularly in male mice. Taken together, these data are not surprising because: 1) CARM1 is critical for maintaining homeostatic cell biology in several, if not all tissues, including the heart and neurons (Fujiwara et al., 2006; Jamet et al., 2022), which in addition to skeletal muscle are important for physical performance; 2) Male CARM1 mKO mice exhibit reduced mobility and run time to exhaustion (vanLieshout et al., 2022); 3) CARM1 protein and mRNA content were higher ($p = 0.07$; data not shown) in the muscle of male mice compared to female mice, although CARM1 activity was similar between sexes; and 4) Differing sex hormone profiles and known sex-specific influences of CARM1 (H. Cheng et al., 2013; Dubois et al., 2012; Frietze et al., 2008; Ikeda et al., 2019; Karakashev et al., 2018; Majumder et al., 2006; Peng et al., 2020) likely play a role in the disparate whole body physiological responses between males and females. In the context of short-term, pharmacological CARM1 inhibition as cancer therapy (Hwang et al., 2021), a temporary lapse in muscle function and performance may be a negligible side effect for an efficacious treatment.

Recent studies have investigated CARM1 during conditions of neurogenic skeletal muscle atrophy (Liu et al., 2019; Stouth et al., 2018, 2020). Our results align with previous data from Liu et al. (2019), as we observed no effect of DEN on CARM1 protein content in the GAST muscle, but 50% greater CARM1 mRNA content ($p < 0.05$; data not shown) 7 days post-DEN in both EZM- and Veh-treated mice. Consistent with this, Stouth et al.

(2018, 2020) observed a significant increase in CARM1 protein content in the TA muscle after 7 days of neurogenic muscle disuse. This nuanced response to DEN between muscles may be due to different CARM1 expression patterns observed across specific skeletal muscles. For instance, in the GAST, PRMT3 and PRMT5 appear to be equally expressed with CARM1, whereas in the SOL, CARM1 is the most abundant PRMT (Wang et al., 2012), although these analyses have not been completed in the TA. We found that CARM1 protein methylation activity was significantly greater in DEN relative to CON muscle as previously reported (Stouth et al., 2020), and as expected, this effect was completely blunted with EZM treatment. However, when investigating the impact of DEN on CARM1 transcriptional target FGFBP1 (vanLieshout et al., 2022), we observed the opposite effect whereby DEN markedly reduced FGFBP1 levels. This finding is concordant with earlier work by Taetzsch and colleagues who observed reduced FGFBP1 expression in skeletal muscles from aged mice and animals with amyotrophic lateral sclerosis (Taetzsch et al., 2017). Taken together, these data lead us to speculate that the transcriptional function of CARM1 in atrophying skeletal muscle may be decoupled from its protein arginine methyltransferase activity. The reduction of FGFBP1 in response to DEN is therefore likely influenced by several factors, including but not limited to CARM1, however, more work is necessary to accurately define this mechanism.

It has previously been shown that the absence of CARM1 in skeletal muscle partially attenuates the loss of muscle mass and size following DEN (Liu et al., 2019; Stouth et al., 2020). We therefore hypothesized that pharmacological CARM1 inhibition would also mitigate neurogenic muscle atrophy. However, neither neurogenic disuse-evoked loss

of skeletal muscle mass and myofibre type-specific CSA, nor fibre type composition were attenuated by CARM1 inhibition, even though EZM treatment was effective at blunting the DEN-induced increase in CARM1 methylation activity in skeletal muscle. Moreover, the response to DEN of the master regulator of mitochondrial biogenesis, PGC-1α, as well as the induction of several representative, canonical markers of the atrophy, autophagy, and muscle protein synthesis programs, was unchanged with CARM1 suppression. We postulate that these disparate findings between CARM1 mKO and EZM treatment are at least partly due to the lack of CARM1 in mKO muscles from inception and ensuing adaptation across the lifespan versus global CARM1 inhibition only in adult mice. For instance, CARM1 is important for embryonic development (Torres-Padilla et al., 2007) and the optimal functioning of muscle progenitor cells (Chang et al., 2018; Kawabe et al., 2012), which likely contributes to reduced muscle mass in CARM1 mKO compared to age-matched WT mice (Stouth et al., 2020; vanLieshout et al., 2022) that was not observed with the CARM1 inhibitor course utilized in the current study. In support of this, using a unilateral TA-specific CARM1 knock down (KD) in mice at 4 weeks prior to DEN, Liu and colleagues observed no difference in muscle mass between the CARM1 KD TA and the contralateral control TA muscle at baseline or 2 weeks post-DEN but found attenuation of mass loss in the CARM1 KD muscle after 4 weeks of DEN (Liu et al., 2019). Thus, we hypothesize that pharmacological CARM1 inhibition could have a similar blunting effect on muscle atrophy following a longer duration of DEN. In our analyses, we combined male and female data in the DEN experiments because sex-specific effects of CARM1 inhibition were not observed under these conditions, which suggests the robust impact of relatively

short-term DEN may supersede more modest effects of sex. Interestingly, pharmacological CARM1 inhibition contributed to a greater DEN-induced reduction in mitochondrial oxidative protein complexes, specifically complexes III and IV. Previous work showed that CARM1 mKO mice have a greater number of grossly distorted mitochondria (vanLieshout et al., 2022). Taken together, CARM1 may play a role in mitochondrial biology in skeletal muscle, and this deserves further investigation given the central role of the organelle in muscle function.

In conclusion, our data demonstrate that pharmacological inhibition of CARM1 is effective at reducing the methyltransferase activity of the enzyme in skeletal muscle. Although blocking CARM1 minimally affected body mass or muscle mass, we found a sex-specific decrease in exercise capacity and muscular endurance such that female mice were less impacted by CARM1 suppression. Additionally, DEN increased CARM1 activity in skeletal muscle of Veh-treated mice, but this was completely blunted by EZM administration. However, the inhibition of CARM1 had no effect on muscle mass, fibre-specific CSA, and atrophy-related signalling following 7 days of DEN, in contrast to previous findings in CARM1 mKO mice (Liu et al., 2019; Stouth et al., 2020). Future studies should use an inducible CARM1 mKO model to address this discrepancy between shorter-term, global pharmacological CARM1 inhibition and the lifelong mKO model. Importantly, despite the modest effects on performance by pharmacologically blocking CARM1, our results indicate that investigations into the use of CARM1 inhibition as a treatment for cancer (Drew et al., 2017; Greenblatt et al., 2018; Hwang et al., 2021;

Mookhtiar et al., 2018; Suresh et al., 2021; D. Wu et al., 2020; Q. Wu et al., 2021) and its related sequelae (e.g., cachectic muscle wasting) should continue.

Acknowledgements

We thank Dr. Mark Bedford (MD Anderson Cancer Center, University of Texas) for the generous gift of the CARM1 substrates antibody. This work was funded by the Natural Sciences and Engineering Research Council of Canada (NSERC), the Canada Research Chairs program, and the Ontario Ministry of Economic Development, Job Creation and Trade (MEDJCT). E.K.W. is an Interdisciplinary Fellow of the Canadian Frailty Network and an NSERC Canada Graduate Scholarship – Master's program scholar. S.Y.N., D.W.S., and T.L.v. are NSERC Doctoral program scholars. A.I.M. is an Ontario Graduate Scholarship recipient. V.L. is the Canada Research Chair (Tier 2) in Neuromuscular Plasticity in Health and Disease and is a MEDJCT Early Researcher.

Author Contributions:

E.K.W. and V.L. conceived and designed the study; E.K.W, S.Y.N., A.I.M., D.W.S., and T.L.v. maintained animal colonies; E.K.W. treated mice, conducted functional tests, performed denervation surgeries, completed laboratory experiments, and analyzed results; S.Y.N. assisted with treatment; T.L.v assisted with functional tests; S.Y.N., A.I.M., and D.W.S., and A.S. assisted with tissue collection, experiments, and analyses; E.K.W. and V.L. drafted and edited the manuscript.

References

Aartsma-Rus, A., & van Putten, M. (2014). Assessing functional performance in the Mdx mouse model. *Journal of Visualized Experiments*. https://doi.org/10.3791/51303

Bedford, M. T., & Clarke, S. G. (2009). Protein Arginine Methylation in Mammals: Who, What, and Why. In *Molecular Cell*. https://doi.org/10.1016/j.molcel.2008.12.013

Bloemberg, D., & Quadrilatero, J. (2012). Rapid determination of myosin heavy chain expression in rat, mouse, and human skeletal muscle using multicolor immunofluorescence analysis. *PLoS ONE*. https://doi.org/10.1371/journal.pone.0035273

Chang, N. C., Sincennes, M. C., Chevalier, F. P., Brun, C. E., Lacaria, M., Segalés, J., Muñoz-Cánoves, P., Ming, H., & Rudnicki, M. A. (2018). The Dystrophin Glycoprotein Complex Regulates the Epigenetic Activation of Muscle Stem Cell Commitment. *Cell Stem Cell*. https://doi.org/10.1016/j.stem.2018.03.022

Cheng, D., Vemulapalli, V., Lu, Y., Shen, J., Aoyagi, S., Fry, C. J., Yang, Y., Foulds, C. E., Stossi, F., Treviño, L. S., Mancini, M. A., O'Malley, B. W., Walker, C. L., Boyer, T. G., & Bedford, M. T. (2018). CARM1 methylates MED12 to regulate its RNA-binding ability. *Life Science Alliance*. https://doi.org/10.26508/lsa.201800117

Cheng, H., Qin, Y., Fan, H., Su, P., Zhang, X., Zhang, H., & Zhou, G. (2013). Overexpression of CARM1 in breast cancer is correlated with poorly characterized clinicopathologic parameters and molecular subtypes. *Diagnostic Pathology*. https://doi.org/10.1186/1746-1596-8-129

Drew, A. E., Moradei, O., Jacques, S. L., Rioux, N., Boriack-Sjodin, A. P., Allain, C., Scott, M. P., Jin, L., Raimondi, A., Handler, J. L., Ott, H. M., Kruger, R. G., McCabe, M. T., Sneeringer, C., Riera, T., Shapiro, G., Waters, N. J., Mitchell, L. H., Duncan, K. W., … Ribich, S. A. (2017). Identification of a CARM1 Inhibitor with Potent in Vitro and in Vivo Activity in Preclinical Models of Multiple Myeloma.

Scientific Reports. https://doi.org/10.1038/s41598-017-18446-z

Dubois, V., Laurent, M., Boonen, S., Vanderschueren, D., & Claessens, F. (2012). Androgens and skeletal muscle: Cellular and molecular action mechanisms underlying the anabolic actions. In *Cellular and Molecular Life Sciences*. https://doi.org/10.1007/s00018-011-0883-3

Egan, B., & Zierath, J. R. (2013). Exercise metabolism and the molecular regulation of skeletal muscle adaptation. In *Cell Metabolism*. https://doi.org/10.1016/j.cmet.2012.12.012

Frietze, S., Lupien, M., Silver, P. A., & Brown, M. (2008). CARM1 regulates estrogen-stimulated breast cancer growth through up-regulation of E2F1. *Cancer Research*. https://doi.org/10.1158/0008-5472.CAN-07-1983

Fujiwara, T., Mori, Y., Chu, D. L., Koyama, Y., Miyata, S., Tanaka, H., Yachi, K., Kubo, T., Yoshikawa, H., & Tohyama, M. (2006). CARM1 Regulates Proliferation of PC12 Cells by Methylating HuD. *Molecular and Cellular Biology*. https://doi.org/10.1128/mcb.26.6.2273-2285.2006

Furrer, R., & Handschin, C. (2019). Muscle wasting diseases: Novel targets and treatments. In *Annual Review of Pharmacology and Toxicology*. https://doi.org/10.1146/annurev-pharmtox-010818-021041

Gould, T. D., Dao, D. T., & Kovacsics, C. E. (2009). The open field test. In *Neuromethods*. https://doi.org/10.1007/978-1-60761-303-9_1

Greenblatt, S. M., Man, N., Hamard, P. J., Asai, T., Karl, D., Martinez, C., Bilbao, D., Stathais, V., McGrew-Jermacowicz, A., Duffort, S., Tadi, M., Blumenthal, E., Newman, S., Vu, L., Xu, Y., Liu, F., Schurer, S. C., McCabe, M. T., Kruger, R. G., … Nimer, S. D. (2018). CARM1 Is Essential for Myeloid Leukemogenesis but Dispensable for Normal Hematopoiesis. *Cancer Cell*. https://doi.org/10.1016/j.ccell.2018.05.007

Guccione, E., & Richard, S. (2019). The regulation, functions and clinical relevance of arginine methylation. In *Nature Reviews Molecular Cell Biology*. https://doi.org/10.1038/s41580-019-0155-x

Hwang, J. W., Cho, Y., Bae, G. U., Kim, S. N., & Kim, Y. K. (2021). Protein arginine methyltransferases: promising targets for cancer therapy. In *Experimental and Molecular Medicine*. https://doi.org/10.1038/s12276-021-00613-y

Ikeda, K., Horie-Inoue, K., & Inoue, S. (2019). Functions of estrogen and estrogen receptor signaling on skeletal muscle. In *Journal of Steroid Biochemistry and Molecular Biology*. https://doi.org/10.1016/j.jsbmb.2019.105375

Jamet, S., Ha, S., Ho, T., Houghtaling, S., Timms, A., Yu, K., Paquette, A., Maga, A. M., Greene, N. D. E., & Beier, D. R. (2022). The Arginine Methyltransferase Carm1 is Necessary for Heart. *G3 Genes|Genomes|Genetics*.

Karakashev, S., Zhu, H., Wu, S., Yokoyama, Y., Bitler, B. G., Park, P. H., Lee, J. H., Kossenkov, A. V., Gaonkar, K. S., Yan, H., Drapkin, R., Conejo-Garcia, J. R., Speicher, D. W., Ordog, T., & Zhang, R. (2018). CARM1-expressing ovarian cancer depends on the histone methyltransferase EZH2 activity. *Nature Communications*. https://doi.org/10.1038/s41467-018-03031-3

Karczewski, K. J., Francioli, L. C., Tiao, G., Cummings, B. B., Alföldi, J., Wang, Q., Collins, R. L., Laricchia, K. M., Ganna, A., Birnbaum, D. P., Gauthier, L. D., Brand, H., Solomonson, M., Watts, N. A., Rhodes, D., Singer-Berk, M., England, E. M., Seaby, E. G., Kosmicki, J. A., … Daly, M. J. (2020). The mutational constraint spectrum quantified from variation in 141,456 humans. *Nature*. https://doi.org/10.1038/s41586-020-2308-7

Kawabe, Y. I., Wang, Y. X., McKinnell, I. W., Bedford, M. T., & Rudnicki, M. A. (2012). Carm1 regulates Pax7 transcriptional activity through MLL1/2 recruitment during asymmetric satellite stem cell divisions. *Cell Stem Cell*. https://doi.org/10.1016/j.stem.2012.07.001

Kim, D., Lee, J., Cheng, D., Li, J., Carter, C., Richie, E., & Bedford, M. T. (2010). Enzymatic activity is required for the in Vivo functions of CARM1. *Journal of Biological Chemistry*. https://doi.org/10.1074/jbc.M109.035865

Kumar, S., Zeng, Z., Bagati, A., Tay, R. E., Sanz, L. A., Hartono, S. R., Ito, Y., Abderazzaq, F., Hatchi, E., Jiang, P., Cartwright, A. N. R., Olawoyin, O., Mathewson, N. D., Pyrdol, J. W., Li, M. Z., Doench, J. G., Booker, M. A., Tolstorukov, M. Y., Elledge, S. J., … Wucherpfennig, K. W. (2021). Carm1 inhibition enables immunotherapy of resistant tumors by dual action on tumor cells and t cells. *Cancer Discovery*. https://doi.org/10.1158/2159-8290.CD-20-1144

Larsen, S. C., Sylvestersen, K. B., Mund, A., Lyon, D., Mullari, M., Madsen, M. V., Daniel, J. A., Jensen, L. J., & Nielsen, M. L. (2016). Proteome-wide analysis of arginine monomethylation reveals widespread occurrence in human cells. *Science Signaling*. https://doi.org/10.1126/scisignal.aaf7329

Liu, Y., Li, J., Shang, Y., Guo, Y., & Li, Z. (2019). CARM1 contributes to skeletal muscle wasting by mediating FoxO3 activity and promoting myofiber autophagy. *Experimental Cell Research*. https://doi.org/10.1016/j.yexcr.2018.11.024

Majumder, S., Liu, Y., Ford, O. H., Mohler, J. L., & Whang, Y. E. (2006). Involvement of arginine methyltransferase CARM1 in androgen receptor function and prostate cancer cell viability. *Prostate*. https://doi.org/10.1002/pros.20438

Manta, A., Stouth, D. W., Xhuti, D., Chi, L., Rebalka, I. A., Kalmar, J. M., Hawke, T. J., & Ljubicic, V. (2019). Chronic exercise mitigates disease mechanisms and improves muscle function in myotonic dystrophy type 1 mice. *Journal of Physiology*. https://doi.org/10.1113/JP277123

Mookhtiar, A. K., Greenblatt, S., Man, N., Karl, D., Stathias, V., Schurer, S., & Nimer, S. D. (2018). CARM1 Inhibition: Evaluation of Response and Efficacy in Acute Myeloid Leukemia. *Blood*. https://doi.org/10.1182/blood-2018-99-114981

Peng, B. L., Li, W. J., Ding, J. C., He, Y. H., Ran, T., Xie, B. L., Wang, Z. R., Shen, H. F., Xiao, R. Q., Gao, W. W., Ye, T. Y., Gao, X., & Liu, W. (2020). A hypermethylation strategy utilized by enhancer-bound CARM1 to promote estrogen receptor α-dependent transcriptional activation and breast carcinogenesis. *Theranostics*. https://doi.org/10.7150/thno.39241

Saleem, A., Carter, H. N., & Hood, D. A. (2014). P53 is necessary for the adaptive changes in cellular milieu subsequent to an acute bout of endurance exercise. *American Journal of Physiology - Cell Physiology*. https://doi.org/10.1152/ajpcell.00270.2013

Sartori, R., Romanello, V., & Sandri, M. (2021). Mechanisms of muscle atrophy and hypertrophy: implications in health and disease. In *Nature Communications*. https://doi.org/10.1038/s41467-020-20123-1

Schmittgen, T. D., & Livak, K. J. (2008). Analyzing real-time PCR data by the comparative CT method. *Nature Protocols*. https://doi.org/10.1038/nprot.2008.73

Stouth, D. W., Manta, A., & Ljubicic, V. (2018). Protein arginine methyltransferase expression, localization, and activity during disuse-induced skeletal muscle plasticity. *American Journal of Physiology - Cell Physiology*. https://doi.org/10.1152/ajpcell.00174.2017

Stouth, D. W., vanLieshout, T. L., Ng, S. Y., Webb, E. K., Manta, A., Moll, Z., & Ljubicic, V. (2020). CARM1 Regulates AMPK Signaling in Skeletal Muscle. *IScience*. https://doi.org/10.1016/j.isci.2020.101755

Suresh, S., Huard, S., & Dubois, T. (2021). CARM1/PRMT4: Making Its Mark beyond Its Function as a Transcriptional Coactivator. In *Trends in Cell Biology*. https://doi.org/10.1016/j.tcb.2020.12.010

Taetzsch, T., Tenga, M. J., & Valdez, G. (2017). Muscle fibers secrete FGFBP1 to slow degeneration of neuromuscular synapses during aging and progression of ALS. *Journal of Neuroscience*. https://doi.org/10.1523/JNEUROSCI.2992-16.2016

Tanida, I., Ueno, T., & Kominami, E. (2008). LC3 and autophagy. *Methods in Molecular Biology*. https://doi.org/10.1007/978-1-59745-157-4_4

Tatem, K. S., Quinn, J. L., Phadke, A., Yu, Q., Gordish-Dressman, H., & Nagaraju, K. (2014). Behavioral and locomotor measurements using an open field activity monitoring system for skeletal muscle diseases. *Journal of Visualized Experiments*. https://doi.org/10.3791/51785

Torres-Padilla, M. E., Parfitt, D. E., Kouzarides, T., & Zernicka-Goetz, M. (2007). Histone arginine methylation regulates pluripotency in the early mouse embryo. *Nature*. https://doi.org/10.1038/nature05458

vanLieshout, T. L., Bonafiglia, J. T., Gurd, B. J., & Ljubicic, V. (2019). Protein arginine methyltransferase biology in humans during acute and chronic skeletal muscle plasticity. *Journal of Applied Physiology*. https://doi.org/10.1152/japplphysiol.00142.2019

vanLieshout, T. L., & Ljubicic, V. (2019). The emergence of protein arginine methyltransferases in skeletal muscle and metabolic disease. In *American Journal of Physiology - Endocrinology and Metabolism*. https://doi.org/10.1152/AJPENDO.00251.2019

vanLieshout, T. L., Stouth, D. W., Hartel, N. G., Vasam, G., Ng, S. Y., Webb, E. K., Rebalka, I. A., Mikhail, A. I., Graham, N. A., Menzies, K. J., Hawke, T. J., & Ljubicic, V. (2022). The CARM1 transcriptome and arginine methylproteome mediate skeletal muscle integrative biology. *Molecular Metabolism*, *64*(July), 101555. https://doi.org/10.1016/j.molmet.2022.101555

vanLieshout, T. L., Stouth, D. W., Tajik, T., & Ljubicic, V. (2018). Exercise-induced Protein Arginine Methyltransferase Expression in Skeletal Muscle. *Medicine and Science in Sports and Exercise*. https://doi.org/10.1249/MSS.0000000000001476

Veazey, K. J., Cheng, D., Lin, K., Villarreal, O. D., Gao, G., Perez-Oquendo, M., Van, H. T., Stratton, S. A., Green, M., Xu, H., Lu, Y., Bedford, M. T., & Santos, M. A. (2020). CARM1 inhibition reduces histone acetyltransferase activity causing synthetic lethality in CREBBP/EP300-mutated lymphomas. *Leukemia*. https://doi.org/10.1038/s41375-020-0908-8

Wang, S. C. M., Dowhan, D. H., Eriksson, N. A., & Muscat, G. E. O. (2012). CARM1/PRMT4 is necessary for the glycogen gene expression programme in skeletal muscle cells. *Biochemical Journal*. https://doi.org/10.1042/BJ20112033

Wu, D., He, J., Zhang, W., Wang, K., Jin, S., Li, J., & Gao, W. (2020). CARM1 promotes non-small cell lung cancer progression through upregulating CCNE2 expression. *Aging*. https://doi.org/10.18632/aging.103280

Wu, Q., Schapira, M., Arrowsmith, C. H., & Barsyte-Lovejoy, D. (2021). Protein arginine methylation: from enigmatic functions to therapeutic targeting. In *Nature Reviews Drug Discovery*. https://doi.org/10.1038/s41573-021-00159-8

Yadav, N., Lee, J., Kim, J., Shen, J., Hu, M. C. T., Aldaz, C. M., & Bedford, M. T. (2003). Specific protein methylation defects and gene expression perturbations in coactivator-associated arginine methyltransferase 1-deficient mice. *Proceedings of the National Academy of Sciences of the United States of America*. https://doi.org/10.1073/pnas.1232272100

Zhang, Z., Guo, Z., Xu, X., Cao, D., Yang, H., Li, Y., Shi, Q., Du, Z., Guo, X., Wang, X., Chen, D., Zhang, Y., Chen, L., Zhou, K., Li, J., Geng, M., Huang, X., & Xiong, B. (2021). Structure-Based Discovery of Potent CARM1 Inhibitors for Solid Tumor and Cancer Immunology Therapy. *Journal of Medicinal Chemistry*. https://doi.org/10.1021/acs.jmedchem.1c01308